

High power fiber lasers: current status and future perspectives [Invited]

D. J. Richardson,* J. Nilsson, and W. A. Clarkson

Optoelectronics Research Centre, University of Southampton, Southampton SO17 1BJ, UK

*Corresponding author: *djr@orc.soton.ac.uk*

Received July 19, 2010; revised August 27, 2010; accepted August 28, 2010;
posted September 10, 2010 (Doc. ID 131957); published October 22, 2010

The rise in output power from rare-earth-doped fiber sources over the past decade, via the use of cladding-pumped fiber architectures, has been dramatic, leading to a range of fiber-based devices with outstanding performance in terms of output power, beam quality, overall efficiency, and flexibility with regard to operating wavelength and radiation format. This success in the high-power arena is largely due to the fiber's geometry, which provides considerable resilience to the effects of heat generation in the core, and facilitates efficient conversion from relatively low-brightness diode pump radiation to high-brightness laser output. In this paper we review the current state of the art in terms of continuous-wave and pulsed performance of ytterbium-doped fiber lasers, the current fiber gain medium of choice, and by far the most developed in terms of high-power performance. We then review the current status and challenges of extending the technology to other rare-earth dopants and associated wavelengths of operation. Throughout we identify the key factors currently limiting fiber laser performance in different operating regimes—in particular thermal management, optical nonlinearity, and damage. Finally, we speculate as to the likely developments in pump laser technology, fiber design and fabrication, architectural approaches, and functionality that lie ahead in the coming decade and the implications they have on fiber laser performance and industrial/scientific adoption. © 2010 Optical Society of America

OCIS codes: 140.3510, 140.3580, 140.5680, 060.2320.

1. INTRODUCTION

Over the last decade powers produced by fiber lasers have shown a remarkable increase, by an average factor of 1.7 each year, corresponding to ~ 2 orders of magnitude over the past decade (Fig. 1), and representing a much steeper increase than that shown by their bulk solid-state counterparts. These increased power levels, with yet higher powers anticipated, are leading to a rapid penetration of fiber systems into applications formerly dominated by other lasers. However, the attraction of fiber lasers goes way beyond the capacity to generate raw optical power, since they possess a number of other physical attributes that distinguish them from other classes of lasers and that differentiate them in terms of functionality, performance, and practicality. These include the following features, all of which have played an important role in establishing the commercial interest and driving the relatively rapid development and practical deployment of fiber lasers:

- Robust single- (transverse) mode operation in mono-mode fibers, giving—in particular—a significant degree of freedom from the thermally induced mode distortions commonly shown by bulk solid-state lasers.
- Broad gain linewidths (up to ~ 20 THz), allowing ultrashort pulse operation, and a wide wavelength tunability.
- Availability of high gains, offering the option of master oscillator power amplifier (MOPA) schemes. In fact, a high power fiber laser system typically consists of a low or medium power master oscillator followed by a high power fiber amplifier.

- Ultrahigh optical and electrical to optical conversion efficiencies.
- Fully fiberized cavities without the need for careful alignment of free-space components allowing for robust and compact system designs.

The aim of this paper is to review the progress made to date toward higher power operation of fiber lasers across a broad range of operation regimes and to look ahead toward the developments and research themes that are likely to shape the further development of the technology over the next decade. The paper is structured as follows. We begin in Section 2 by providing a review of the current state of the art in terms of high power continuous-wave (cw) operation—as best exemplified by progress in the field of ytterbium-doped fiber-based laser (YDFL) systems, which are currently the preferred gain media by virtue of their efficiency, broad gain bandwidth, and operational wavelength around 1060 nm. In Section 3, we review progress in pulsed-fiber-laser performance, again largely in the context of YDFLs, but with the emphasis being to illustrate the broad range of operational modes that are possible using fiber laser technology. In Section 4, we complete our summary of the current state of the art by describing progress in terms of power scaling of fiber lasers operating on other rare-earth (RE) transitions and in particular those that allow the generation of laser light at important longer nominally eye-safe wavelengths around 1550 and 2000 nm. Our intention throughout these sections is not to be rigorously complete in terms of reviewing the existing state of the art, as the space available simply precludes this. Rather, we look to providing a

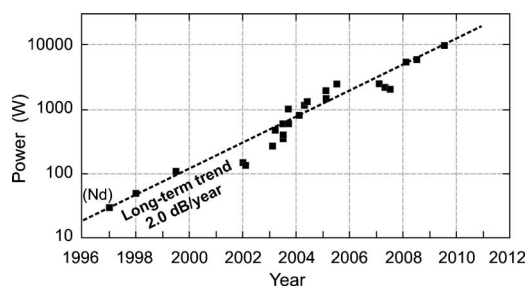


Fig. 1. Progress in output power from diffraction-limited and near-diffraction-limited fiber lasers. Since 1999, all results are with Yb-doped fibers.

high level overview of the technology that will be accessible to the non-fiber specialist and identify the key issues that will likely ultimately limit the performance in different operational regimes. Furthermore, despite the length of this paper, there are many important aspects and advances we have not included, e.g., when it comes to fiber composition and fabrication. Photodarkening is particularly important, and we refer the interested reader to the literature.

In Section 5, finally, we attempt to look ahead and provide a personal view as to how the technology is likely to evolve in the light of technological advances in relevant underpinning areas and speculate as to the new fibers, system concepts, and architectures required to continue to extend the performance envelope on all fronts over the coming decade. Fiber lasers are optically pumped, and this makes the development of semiconductor pump sources particularly important. We draw our conclusions in Section 6.

2. STATE OF THE ART—CONTINUOUS-WAVE FIBER LASERS

High power YDFLs have been described in detail in several publications [1–6], and our aim here is to concentrate on the most important points. The first operation of a fiber laser, in the early 1960s, was demonstrated by Snitzer and co-workers [7–9] and revisited in the 1970s by Stone and Burrus [10], before major interest was rekindled in 1985 due largely to the efforts of Payne and co-workers [11,12]. Their work on neodymium-doped fibers revealed the potential for optical gains of several decibels per milliwatt of absorbed pump power. Consequently, even with a modest pump power of a few milliwatts, provided by cheap and by then readily available laser diodes (LDs), levels of optical gain could be reached that were highly promising for applications such as optical telecommunication amplifiers. In that context, interest was focused on the erbium-doped fiber amplifier [13], whose operating wavelength of $\sim 1.55 \mu\text{m}$ falls in the third telecommunication window. This was of immense importance, because no solution existed at the time for this huge application. The impact on telecommunications of this work has been profound, leading to the development of the Internet as we know it today. Besides the excitement about telecommunication amplifiers there was also considerable interest in fiber lasers, as they offer a number of attractive features when compared to other lasers. Now, nearly 50

years after the initial demonstration, and 25 years from their renaissance, cw fiber lasers, specifically silica-host YDFLs, have reached 10 kW in the single-mode (SM) regime [14]. This is one order of magnitude higher than for other single-mode fiber sources. The attractions and potential of Yb-doped fibers had been recognized by Hanna and co-workers in 1990 [1,2,15]. These include a broad gain bandwidth, with operation from 975 nm [15–18] to 1180 nm [19] demonstrated in different devices. While YDFLs work best between 1060 and 1100 nm, laser operation even at these extreme wavelengths has been scaled to a very respectable 100 W and above. A tuning range of 110 nm has been achieved at the watt level [20], and as much as 152 nm at lower power [15].

Another attraction is the broad absorption band extending from 900 to 980 nm, covering wavelengths at which high power pump LDs are at their best. The absorption further extends out to 1050 nm, which allows tandem-pumping (in-band pumping with high-brightness pump sources) [14,21] at wavelengths close to the emission wavelength. Figure 2 shows the absorption and emission spectra of Yb-doped silica fiber. Additional spectroscopic attractions include a long, 1 ms, metastable state lifetime and a simple energy level structure with only two $4f$ energy levels, which benefits energy storage and allows the use of high doping concentrations. In addition, as with other RE dopants, the fiber geometry facilitates low laser thresholds, high gain efficiency, and high gain. These features have paved the way for power scaling in a wide range of fiber-based devices.

A. Power Scaling of Ytterbium-Doped Fiber Sources

It is for high powers, though, that YDFLs are most renowned. Since 1999, the record-breaking near-diffraction-limited fiber lasers shown in Fig. 1 have all been Yb-doped. Yb's superior power-scaling properties stem from an exceptionally low quantum defect for LD pumping at $9\mu\text{x}$ nm, and thus a low thermal load, as well as high permissible dopant concentrations and thus high pump absorption per unit length. These are both important factors for power scaling of fiber lasers, with the thermal management greatly further simplified by the fiber geometry. Nonlinearities and damage are equally important factors. These are easiest to avoid in cw operation, and consequently the record-breaking lasers in terms of the average power have all been cw.

Three key technologies underpin Yb-doped as well as other high power RE-doped fiber lasers: One is low-loss

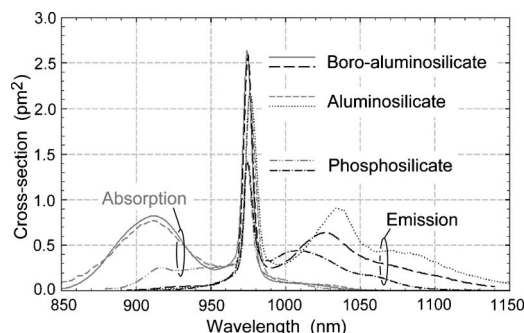


Fig. 2. Emission and absorption spectrum of ytterbium ions in different silica hosts.

doping with RE ions [7]. The other two are directly related to pumping, reflecting its importance for power scaling. They are high power multimode (MM) LDs [22] and double-clad fibers, which open up the option of cladding-pumping [23–25]. Cladding-pumped fiber lasers have proven to be remarkably scalable and have been the platform for the impressive rate at which the power has increased over the last two decades, following the initial demonstration in 1988 [25]. The essence of this double-cladding approach is that the active RE-doped core is surrounded by a much larger “inner cladding” (see Fig. 3). The pump beam is launched into the inner cladding and confined within it by an outer cladding, which surrounds the inner cladding. The pump is then progressively absorbed into the core as it propagates along the fiber. Thereby, a MM pump can efficiently pump a monomode core and produce a single-mode fiber laser output. Thus, by means of rather simple and robust configurations (see Fig. 4) one achieves a large enhancement of the fiber laser’s beam brightness compared to that of the pump. Cladding-pumped YDFLs allow for up to 6 orders of magnitude brightness enhancement, and close to 5 orders have been demonstrated experimentally [3,5,26], although 3–4 orders are more typical. This stems from the larger spatial and angular pump acceptance [represented by the product of area and the square of the numerical aperture (NA)] for the inner cladding compared to that of the core. Since brightness is the relevant figure of merit for so many applications, the relative ease with which fiber lasers have achieved this brightness enhancement at high power has been the stimulant for a widespread and rapid increase in efforts on fiber laser development, leading to the improvements illustrated in Fig. 1 and many other impressive results besides those. As a result, high power fiber lasers are now the leading contenders for many important scientific and industrial applications.

From a historical perspective it is worth saying that the initial aspirations of cladding-pumped fibers were considerably more modest, for example, targeting telecommunication amplifiers at 1.5 μm at the sub-watt level [27]. The output power in those days was largely limited by the power and availability of pump diodes with beam quality good enough for launch into the double-clad fibers. The low pump brightness favored the use of gain media with low thresholds, including Er:Yb co-doped silica emitting at 1.5–1.6 μm . In these, a high Yb-to-Er concentration ratio increases the pump rate of the Er ions [28,29]. Nd is a four-level system when emitting at ~ 1060 nm, with an even lower laser threshold. Combined with the relatively

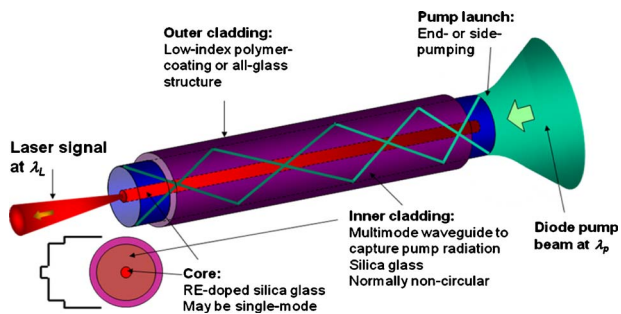


Fig. 3. (Color online) Principle of cladding-pumping.

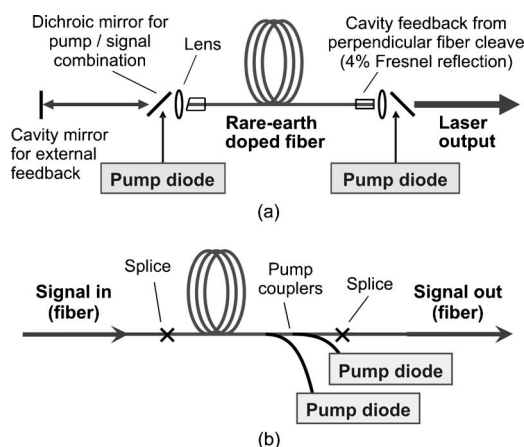


Fig. 4. Schematic of a (a) cladding-pumped fiber laser and (b) fiber amplifier in free-space end-pumped and all-fiber side-pumped configurations, respectively.

advanced state of diodes for the pumping of Nd:YAG at 808 nm, this made Nd the dopant of choice for early high power fiber lasers [30].

Today’s high power pump diodes are sufficiently bright to make threshold considerations largely unimportant for most high power fiber lasers. However, there are exceptions, with the fiber disk laser being a prominent example [31]. This operates with a relatively low pump intensity and uses a highly MM Nd-doped core to enhance the pump absorption efficiency. The first kilowatt-level MM fiber laser was demonstrated in 2002 using this architecture with three cascaded high power gain blocks [31].

Despite this impressive result, Nd-doped fiber lasers in this wavelength range have largely been sidelined by Yb, following the advent of high-brightness 9xx nm pump diodes. These overcame the hurdle of ytterbium’s higher threshold and brought out the advantages of a lower quantum defect and, crucially, a higher quench-free concentration. The demonstration of the first single-mode Yb-doped fiber laser with over 100 W of output power in 1999 [32] served as convincing evidence of these advantages and a sign of the progress that was to come. This laser used a fiber with relatively small inner cladding and core, which—as one would suspect—brought both the diodes and the fiber relatively close to their limits, e.g., in terms of diode damage and fiber nonlinearities. Nevertheless, this important demonstration illustrated that the basic technology was in place to allow for a rapid increase in the average power by scaling the size of the optical fiber and the pump diode source. Soon thereafter, the cladding-pumped fiber laser reached the kilowatt level [33], using a simple YDFL end-pumped by diode stacks. Following refinements of the large-area core design and fabrication, single-mode operation was demonstrated as well [3], something which would not have been possible with Nd doping. These Yb-doped fibers had inner-cladding diameters (for the pump waveguide) of almost 1 mm and core diameters of around 40 μm [3,5,33]. Thus, the inner-cladding-to-core area ratio was around 400, and the output beam was up to 5 orders of magnitude brighter than the diode pump beam. The fiber length was in the region of 10 m.

Commercial devices at the kilowatt level and above tend to use an architecture that is different to a free run-

ning laser. Instead of generating all the output power in a single fiber stage, they often use one or more high power amplifier stages that are seeded by a medium- or even high power fiber oscillator. Optical pumping is typically engineered around a large number of single-emitter or few-emitter diode sources pigtailed with 100 μm fibers. These are then combined to achieve high power in a fiber network before being launched into the RE-doped fiber using sophisticated fiber arrangements which are often proprietary. Examples include SPI Lasers' approach (GT-Wave technology [34,35]) as well as IPGs [36].

The highest power diffraction-limited YDFs have used yet another level of sophistication, namely, tandem-pumping. Tandem-pumping, in which one or several fiber lasers pump another one [14,21], offers several advantages for power scaling. In particular it makes it possible to pump close to the emission wavelength so that the quantum defect heating can be low resulting in a reduced thermal load. IPG's 10 kW fiber laser [14] was pumped by YDFs at 1018 nm and emitted at 1070 nm, for a quantum defect of less than 5%, which is roughly half of that of a directly diode-pumped YDFL. The high pump brightness possible with tandem-pumping also allows for a reduction in the dimension of the inner cladding required to reach high power levels—it is possible to launch sufficient diode power into a thick but realistic Yb-doped fiber to reach the 10 kW level given the brightness of current state-of-the-art pump diodes [5]; however, it is quite challenging. This becomes much easier with tandem-pumping, although one difficulty is to maintain the high brightness of the pump inside the pumped YDF, i.e., to guide the pump in a small inner cladding. This may not be strictly necessary, but improves the pump overlap with the core, which shortens the absorption length. Thus, although direct diode-pumping looks scalable to 10 kW [5], all double-clad fiber lasers at 3 kW and above have in fact been tandem-pumped, as far as we know.

B. Single-Frequency Ytterbium-Doped Fiber Sources

The fiber lasers considered so far in our discussion, e.g., in Fig. 1, have been relatively broadband devices with linewidths typically in the 1–10 nm range. In such devices, in the cw regime, nonlinear scattering—stimulated Raman scattering (SRS) in the first instance—is a weak effect. It is relatively easy to avoid and can often be disregarded, except at the highest powers and with long delivery fibers. However, some applications benefit from the much narrower linewidth that can be provided by single-frequency sources. One important example is coherent beam combination of multiple high power single-frequency fiber sources [37]. This scheme offers the prospect of very high powers, and consequently this has stimulated much interest in single-frequency power scaling. In the high power regime, a single-frequency fiber source is typically configured as a high-gain MOPA seeded by a lower power oscillator as shown in Fig. 5. This configuration avoids the stability problems of a high power single-frequency oscillator and takes advantage of the high gain, high power, and high efficiency that fiber amplifiers can provide, all at the same time. Stimulated Brillouin scattering (SBS) [38–40] is the dominant nonlinearity for such devices [41], particularly at linewidths

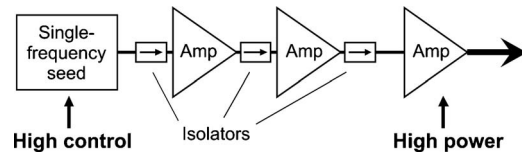


Fig. 5. Schematic of a typical single-frequency fiber MOPA.

smaller than ~ 10 MHz. SBS is nominally around 500 times stronger than SRS, making it a severe obstacle for high power single-frequency fiber sources that needs to be addressed for power scaling. Short fibers with a large mode area (LMA) core design help to suppress nonlinearities, including SBS, and allow scaling to the hundred-watt regime [42]. This is a respectable power, but still less than competing technologies. This means that, without further SBS suppression, fibers would be a rather poor choice for high power single-frequency sources in many cases. However, if SBS can be suppressed then fiber systems offer many advantages. Fortunately, the Brillouin nonlinearity is subtler and more complex than the Raman nonlinearity, involving a propagating acoustic wave, and is amenable to manipulation and indeed suppression. This has been the focus of considerable recent research. There are several options for SBS manipulation and mitigation, including straining the fiber in order to broaden the gain bandwidth [43] and signal linewidth broadening [44] (if the application allows). The broadening should exceed the intrinsic linewidth of SBS to be significant (a few tens of megahertz at 1–1.1 μm), while a linewidth of a few tens of gigahertz may be required to completely suppress SBS beyond 1 kW.

Since the speed of sound is temperature-dependent, the longitudinal temperature variations that occur naturally in a high power fiber amplifier also help to broaden and thus suppress SBS [45]. Thermal broadening has been the most important effect in the progress in single-frequency power scaling to date allowing the kilowatt level to be reached [46]. Higher powers still have been obtained by applying modest spectral broadening to the signal. Thus, 1.7 kW was reached by applying a modest 400 MHz phase modulation to the signal and accepting a slightly degraded beam quality ($M^2=1.6$) [46]. The larger effective mode area of the fiber in this demonstration also helped to suppress SBS. This result represents the highest power high-gain fiber amplifier reported to date, and serves as a convincing demonstration of the ability of fiber sources to simultaneously provide high control, high gain, high efficiency, and high power.

Another interesting approach for the SBS suppression is to manipulate the propagation of the acoustic wave by making the fiber core an acoustic antiguide in order to reduce the acousto-optic (AO) interaction [47–50]. A 10 dB suppression of the Brillouin gain has been realized via this technique [50], with theoretical optimization of the antiguide suggesting that 15 dB may be possible [51]. However, the challenges of implementing an acoustic antiguide in an ytterbium-doped fiber, with all its additional requirements on concentration, resistance to photodarkening, etc., should not be underestimated; and so far, this approach has not yielded better performance than simple longitudinal thermal broadening.

3. STATE OF THE ART—PULSED FIBER LASERS

One of the great attractions of fiber laser technology, in addition to the high average powers that can be achieved, is the diversity of temporal output properties that can be supported. Due to the very large spectral bandwidths achievable from RE ions in glass, fiber lasers can be built to operate from the cw regime down to pulse durations of just a few femtoseconds.

A. Scaling Peak Power and Pulse Energies

To emphasize the flexibility of fiber technology in Fig. 6 we show a diagram indicating the fiber-based pulsed generation approaches best suited to generate a given combination of pulse duration and pulse repetition frequency (PRF). Examining the horizontal plane we see that a fiber-based approach exists for almost any desired combination of performance specifications. For example, the options for low (kilohertz) frequency trains of nanosecond pulses include Q-switching [52] and external modulation of a cw laser [53], sub-100 fs operation can be achieved by passive fundamental mode locking at frequencies up to a few hundred megahertz [54,55], and active harmonic mode locking can yield picosecond pulses at many tens of gigahertz repetition rate [56]. Additional techniques such as external cavity compression in fiber [57] or harmonic-passive mode locking [58] can then be used if required to extend these basic techniques to achieve shorter pulses and higher repetition rates, respectively. Time gating using fast modulators can be used to reduce the repetition rates to any desired sub-harmonic of the fundamental repetition rate. Ultrahigh frequency trains of pulses (>40 GHz) can be generated either by time division multiplexing of lower frequency sources or by nonlinear optical techniques in which a high frequency sinusoidal signal (e.g., generated by beating together two lasers with different frequencies) is reshaped into a train of pulses at the corresponding frequency using soliton compression effects [59]. The diagram should not be taken too literally; in reality the boundaries between approaches are not well

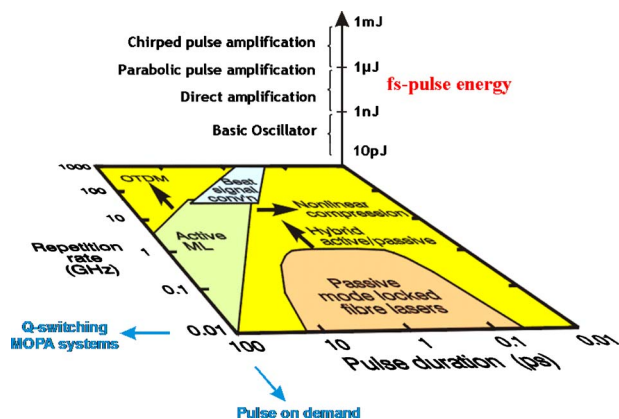


Fig. 6. (Color online) Diagram illustrating (in the horizontal plane) fiber-based pulse generation techniques appropriate to a given operational regime (in terms of repetition rate versus pulse duration). The vertical axis lists the pulse amplification techniques required to access particular pulse energy regimes for femtosecond pulses (OTDM, optical time division multiplexing; Active ML, active mode locking).

defined, and there are often several options to address a given pulse duration and PRF range. Nevertheless it serves to highlight the fact that fiber-based approaches allow the generation of a very broad range of pulsed formats—arguably very much wider than for more conventional and established technologies, such as semiconductor or bulk solid-state lasers.

The real benefits of the fiber approach though only really emerge when combining the basic source capability described above with the use of the fiber MOPA concept since this allows for significant scaling of both the peak and, arguably most significantly, average power levels. The challenge with power scaling is to preserve the desired seed laser properties during the amplification process in the face of the various deleterious effects such as fiber nonlinearity, chromatic dispersion, gain saturation, birefringence, and thermal beam distortions that otherwise degrade the spectral, temporal, and spatial fidelities of the signal. Moreover, to ensure reliable system operation, it is obviously necessary to avoid all-fiber and component damage mechanisms. This becomes progressively more of a challenge as the peak and average power levels are increased, resulting in the need to adopt progressively more complex mitigation strategies. To emphasize this fact we illustrate the different and progressively more elaborate forms of pulse amplification needed to achieve various levels of pulse energy for femtosecond pulses on the vertical axis in Fig. 6. Using approaches such as parabolic and chirped pulse amplification (CPA), which we shall describe in more detail shortly, it is possible to boost the pulse energies achievable from a simple femtosecond fiber oscillator by more than 6 orders of magnitude: from the nanojoule to the millijoule regime.

From the perspective of pulsed fiber systems, the primary performance metrics are output peak power, pulse energy, pulse duration, and repetition frequency. The average power is defined by the product of pulse energy and repetition rate, and the pulse energy by the peak power, pulse duration, and detailed pulse shape. The limitations to pulsed system performance are ordinarily set either by energy extraction limits (generally a dominant consideration only in the case of pulses longer than ~ 1 – 10 ns as we shall discuss later) or, more frequently, by the peak power. With regard to the peak power, the limitation may be defined by

(a) a maximum tolerable degree of nonlinear distortion [e.g., as characterized by an acceptable nonlinear phase shift induced by self-phase modulation (SPM) or a tolerable level of energy transfer to other wavelengths by inelastic scattering due to either SRS or SBS]. Note that the strengths of all of these nonlinear effects scale either linearly (for SPM) or exponentially (for SRS and SBS) in proportion to fiber length and power, and in inverse proportion to the mode area [40];

(b) optical damage limits (which for most single-mode fibers scale in inverse proportion to mode area [60,61]);

(c) or, as we enter the megawatt peak power regime, by self-focusing (which depends only on the total power flow within the fiber, and which is typically negligible up until the peak power exceeds a certain threshold—around 4 MW at a wavelength of 1060 nm [62]).

Exactly which of these above limitations dominates in a given system depends on the pulse duration and the specifics of the laser architecture. However, the importance of developing fibers providing LMAs and high gains per unit length should be obvious. Consequently, this has become a topic of intense research interest over the years. Unfortunately, the use of a larger core poses a challenge to the maintenance of single-mode operation and often compromises need to be struck between brightness, practicality, and stability. The key issues include the practicalities of bending, the presence of increased bend loss, and the tendency to higher-order mode (HOM) operation. Moreover, as the larger diameter fiber progressively resembles a bulk solid-state laser, so the raft of problems associated with heat removal, all very familiar to bulk lasers, also start eventually to impact fibers. Indeed, one of the most striking achievements in the development of high power fiber lasers has been the extent to which it has proved possible to reconcile the various conflicting requirements, drawing greatly on the resources of fiber designers and fabricators alike. There is still some room for further advances in power levels before these difficulties dominate, but the success here will depend increasingly on a detailed understanding of the limiting mechanisms and of ways to circumvent them. We will return to a more detailed discussion of mode area scaling in Section 5; for the present suffice it to say that achieving a robust single-mode performance in a core with an effective mode area larger than $1000 \mu\text{m}^2$ at $1 \mu\text{m}$ is currently proving challenging within commercial systems (although it is to be appreciated that around 1 order of magnitude larger mode areas have been reported in the laboratory using highly advanced fiber designs (see Section 5). Note that one major further advantage of using large-core fibers is that they provide for greater pump absorption per unit length. This allows for considerably shorter devices and represents a significant further benefit beyond just reduced intensities for the mitigation of nonlinear effects.

With regard to fiber damage limits due to high peak power the standard approach to estimating damage thresholds in the pulsed regime is to use the data and bulk damage limits defined in the paper by Stuart *et al.* for pure fused silica [60]. According to this paper the bulk damage threshold P_{max} for pulses with a duration τ between 50 ps and 100 ns can be estimated via the following expression:

$$P_{\text{max}} = I_{\text{th}} A_{\text{eff}} = \frac{XA_{\text{eff}}}{\sqrt{\tau}}, \quad (1)$$

where $X = 150 \text{ GW ns}^{0.5}/\text{cm}^2 = 1.5 \text{ kW ns}^{0.5}/\mu\text{m}^2$, and τ is expressed in nanoseconds. This result is based on systematic measurements made at a wavelength of $1.06 \mu\text{m}$. This $\tau^{-0.5}$ dependence is a result of the fact that for pulses longer than 10 ps, the damage is thermal (melting/boiling) in origin, with a limiting rate determined by heat diffusion from conduction band electrons to the lattice. For pulses shorter than ~ 10 ps, ablation takes over as the primary damage mechanism, and a weaker dependence on the pulse duration then ensues as shown in [61]. We note also that Eq. (1) can be rewritten as $EP_{\text{max}} \leq 2.25 \text{ mJ W}/\mu\text{m}^4$, where E is the pulse energy. This

shows that in this damage-limited regime, a higher peak power has to be traded for a lower pulse energy, and vice versa.

In principle, one might expect the surface damage threshold of fiber to be similar to that of bulk silica and with appropriate end facet preparation (e.g., laser-cleaving) the observed threshold for fiber does appear to approach this. However, in practice the facets are the weakest points, and depending on the facet termination quality the surface damage threshold might typically be a factor of 2–10 down on the bulk threshold. In order to mitigate against surface damage it is normal to splice coreless end-caps to the end of the fiber. This allows the beam to expand within the bulk glass prior to reaching the surface, where the intensities are now substantially reduced. Note that few studies have been reported on damage mechanisms in the cw regime where power densities for damage are frequently quoted, but with little if any quantitative justification. The current “wisdom” is that the cw damage threshold for fibers is around $10\text{--}20 \text{ W}/\mu\text{m}^2$ at $1.06 \mu\text{m}$ for ytterbium-doped fibers, but there is a genuine need for systematic studies in this direction.

Although we have chosen to provide indicative numbers for damage thresholds for fiber lasers, we would not like to give the impression that ensuring that the nominal specification of the laser is such that the intensities appear to be well below these levels eliminates all damage concerns. This is most certainly not the case. Fiber lasers and amplifiers are subject to instabilities and modes of self-pulsation under certain different operating conditions which can have catastrophic repercussions. YDFLs are particularly notorious in this regard. For example, failure to adequately seed an ytterbium fiber amplifier can result in the formation of intense pulses with energies sufficient to shatter, or even vaporize, the fiber core over considerable length scales and to destroy all inline components in the process (often the pump lasers also). Fiber fuse effects [63] can also be of concern, even at relatively modest average powers of just a few watts, unless appropriate care is taken with thermal management. The fiber fuse results in a traveling hot spot that slowly propagates along the fiber destroying the core as it goes. To date little work has been reported in the open literature on damage mechanisms within fiber laser systems.

To illustrate the favored current approaches applicable to specific pulse duration regimes, we consider separately the current status of fiber pulse sources in the nanosecond and ultrashort (picosecond to femtosecond) regimes.

B. Nanosecond Fiber Laser Sources

The most common and straightforward way to generate nanosecond pulses within a fiber laser is to use Q-switching. This requires the incorporation of some element within the cavity that switches the cavity loss from as a high as possible a value, to as low as possible a value over a suitably short time scale. Both active and passive switching elements have been used to this effect. The minimum pulse durations from Q-switched fiber lasers are just a few nanoseconds, although pulse durations of the order or tens to hundreds of nanoseconds are more typical for cladding-pumped devices.

Active Q -switching is most commonly achieved in fiber laser cavities using bulk AO devices to modulate the cavity loss [64–66]. AO devices have sufficiently fast switching responses (rise time of the order 10–100 ns) and operate at sufficiently high repetition rates (from pulse on demand up to 1 MHz or so) to be appropriate for the pump rates and metastable lifetimes [intrinsically 10 μ s–10 ms, although the actual lifetime is significantly shortened by amplified spontaneous emission (ASE)] for the RE transitions of interest. AO devices also provide for very good extinction ratios (>50 dB) and diffraction efficiencies (>85%) when operating the laser on the first diffraction order. There have been several reports of Q -switching using fiber-based AO devices [67,68], rather than bulk optic components. However, while these might allow for more compact and lower-loss cavities, the performance achieved in terms of pulse energy and minimum pulse duration has generally been inferior to that achieved with bulk AO components. Passive Q -switching is another attractive option in that it is simple and requires no complex drive electronics or expensive active optical componentry. Various approaches to passively Q -switched fiber lasers have been demonstrated in the literature based on a number of different material approaches and which include, for example, the use of crystals such as $\text{Co}^{2+}:\text{ZnS}$ [69], $\text{Cr}^{4+}:\text{YAG}$ [70], and semiconductor saturable absorbers [71]. Unfortunately, the extinction ratios that can be achieved using passive saturable absorbers, while sufficient to initiate stable self-pulsation, generally do not allow for sufficient gain hold-off to permit the generation of particularly high-energy pulses, unless longer or cascaded devices are used [72].

It has been shown that the maximum energy that can be extracted from fiber lasers and amplifiers is around ten times the intrinsic saturation energy E_{sat} , given simply by

$$E_{\text{sat}} \approx h\nu_L A_{\text{co}} [\sigma_a(\lambda_L) + \sigma_e(\lambda_L)] \eta_L = E_{\text{fluence}} A_{\text{co}}, \quad (2)$$

where $h\nu_L$ is the photon energy at the laser wavelength, A_{co} is the core area, η_L is the spatial overlap factor for the lasing mode with the doped core, and $\sigma_a(\lambda_L)$ and $\sigma_e(\lambda_L)$ are the absorption and emission cross-sections, respectively, at the laser wavelength λ_L [73]. The primary thing to note is that the saturation energy is proportional to the core area. The saturation fluence E_{fluence} of Yb is around 0.5 $\mu\text{J}/\mu\text{m}^2$. Given our previous comment on the maximum practical mode area, this means that pulse energies of a few millijoules should be achievable in a diffraction-limited beam from fiber lasers based on state-of-the-art LMA fibers. This is indeed consistent with the current experimental status in nanosecond Q -switch pulsed fiber laser systems [65,66]. By reducing the beam quality and working with larger core structures, pulse energies of tens of millijoules should be achievable and have indeed been reported [74]. While these levels of pulse energy may perhaps be considered small as compared to the joules achievable from bulk lasers, it is still appreciable and sufficient for a large number of applications—most notably marking and precision machining. As a consequence, given their many advantages over existing laser technologies, fiber lasers are now being used extensively in these areas.

Although Q -switching offers the benefit of simplicity, it does not provide for a great deal of control of the output temporal pulse shape. As a consequence the great majority of nanosecond pulsed fiber systems on the market employ a MOPA-based approach in which the seed laser may itself be a Q -switched fiber laser, a directly modulated diode laser, or an externally modulated cw laser. Note that much of the early work on nanosecond MOPAs was actually conducted on core-pumped erbium-doped fiber allowing pulse energies approaching 0.5 mJ and peak powers well in excess of 100 kW [53,75] to be achieved with very modest (~ 1 W) levels of pump power. The adoption of cladding-pumping has subsequently allowed further scaling of the average powers, repetition rates, and (to a lesser extent) pulse energy [76].

One of the most exciting possibilities of the pulsed MOPA is to exploit the rapid modulation possibilities of fast electro-optic modulators (EOMs) or electro-absorption modulators (EAMs), or alternatively directly modulated diodes, to allow adaptive pulse shaping [77,78]. This allows the creation of designer pulse shapes optimized for a particular end application. For example, in our laboratories we have demonstrated a pulsed system capable of generating multi-millijoule shaped pulses at power levels as high as 300 W in an end-pumped high power system [79], and over 100 W within a fully fiberized system [80], and have successfully used these in both materials processing and frequency conversion experiments. Both systems were pump power limited, and scaling to much higher average powers and pulse repetition rates should certainly be possible. Before moving on it is worth noting that significant results have been made in the nanosecond regime with regard to peak power scaling with peak powers approaching 4 MW recently reported for 1 ns pulses using very large mode area fiber amplifiers based on rod-type fibers (see Section 5) [81]. These peak powers are right at the nonlinear limit imposed by self-focusing.

C. Ultrashort Pulse Operation

RE-doped optical fibers with their broad gain bandwidths provide convenient media for the generation and amplification of short optical pulses. For example the ~ 100 nm gain bandwidth achievable in an ytterbium-doped fiber should be capable of supporting pulses shorter than 20 fs. As well as providing gain, optical fibers also possess both nonlinearity and dispersion, and these characteristics have to be considered for short pulse applications. These properties can be varied substantially by fiber design or by the choice of operating wavelength. In certain instances, these properties can be used to good effect, for example, to initiate mode locking. In other instances they can have a deleterious effect, restricting—for example—the peak power of the pulses that can be generated or, alternatively, the pulse quality that can be obtained. Pulses can be generated either through passive mode-locking techniques or by active modulation of the intracavity field. Active techniques are generally more suited to the generation of picosecond pulses at high repetition rates, while passive techniques are generally suited to the generation of ultrashort pulses. Note that single cycle pulses

with durations as short as 4.5 fs have now been demonstrated using a fiber laser [82].

The limits imposed on the amplification of ultrashort pulses are generally defined by peak power considerations rather than energy storage. Typically, spectral distortion due to SPM reduces the quality of pulses and can be taken as the fundamental measure of how much nonlinearity can be tolerated by a pulse propagating within an amplifier. Nonlinear Kerr effects are characterized by the nonlinear coefficient n_2 which defines how the refractive index of the core glass material varies with intensity. Nonlinear refraction then results in short optical pulses, generating increased optical bandwidth through SPM as they propagate through a fiber. This degrades pulse quality and limits their utility. A pulse of power profile $P(t)$ generates an instantaneous phase $\phi(t)$ across the pulse envelope. In a uniform fiber of length L without loss or gain the expression for this phase is given by

$$\phi(t) = \frac{n_2 k L P(t)}{A_{\text{eff}}}, \quad (3)$$

where A_{eff} is the effective mode area, and $k = 2\pi/\lambda$. For a pulse propagating along an amplifier experiencing a uniform logarithmic gain per unit length G , L in Eq. (3) should be replaced with an effective length L_{eff} (with reference to the amplifier output power) given by

$$L_{\text{eff}} = \frac{1}{G}(1 - e^{-GL}). \quad (4)$$

If we set a maximum nonlinear phase shift of 2π at the pulse peak as roughly representative of the maximum SPM that can be tolerated, and assume an effective amplifier device length of, say, 20 cm, then we can estimate a maximum peak intensity of order 100 kW for direct pulse amplification in a relatively standard 30 μm core LMA fiber. For a 10 ps pulse this corresponds to a maximum pulse energy of order 1 μJ and for a pulse of 100 fs around 10 nJ. Using state-of-the-art LMA fibers a further order of magnitude increase in pulse energy and peak power is possible using direct pulse amplification—resulting in peak powers of order 1 MW [83,84]. Just as in the nanosecond regime, the peak powers are encroaching upon the self-focusing limit in the ultrashort pulse regime in simple system configurations.

1. Picosecond Fiber Lasers

Actively mode-locked fiber lasers, gain-switched or mode-locked semiconductor lasers, or even cw lasers externally modulated with fast EOMs or EAMs can all be used to generate trains of picosecond pulses. Repetition rates ranging from a pulse on demand through to tens of gigahertz are possible using an appropriate choice of technology.

These compact sources can then be used as seeds for direct amplification to very high average power levels in a fiber MOPA. For example, we recently reported a 320 W average power system based on the direct amplification of a simple gain-switched 1060 nm semiconductor laser operating at frequencies in the range 0.1–1 GHz [85]. The output pulse duration was around 20 ps with peak powers in excess of 20 kW generated. Such sources, offering a

combination of high peak and average powers in a quasi-cw regime, are particularly interesting from the perspective of onward frequency conversion, e.g., to the visible spectral region through second-harmonic generation [86] or supercontinuum generation [87] and to the mid-IR using optical parametric oscillators [88]. Using state-of-the-art leakage channel fibers directly amplified 10 ps pulses with a peak power in excess of 1 MW were recently reported [84].

2. Femtosecond Fiber Lasers

To get to higher pulse energy levels for femtosecond-MOPA schemes it is necessary to implement more advanced external pulse amplification approaches such as those discussed below. Clearly this adds complexity, and the pulse energies ultimately achievable are still lower than possible with bulk laser approaches due to nonlinearity and dispersion in the long lengths of fibers involved. However, the average power levels achievable, with reported values in excess of 830 W [89], represent 2–3 orders of magnitude increase over the existing technology. This can be exploited in a variety of ways, for example, to increase materials processing speeds and imaging rates in several fields of application. We review the two primary forms of external pulse amplification below.

(a) *Parabolic pulse amplification*: It has been shown that by amplifying short pulses in fiber with normal dispersion, it is possible to form self-similar pulse solutions that are characterized by the steady development of a linear chirp across the pulse form, as it is amplified within the fiber [90,91]. The self-similar pulses that develop are parabolic in shape, and thus this technique has become known as either parabolic or similariton pulse amplification. The pulse consequently broadens in time as it is progressively amplified, thereby spreading the pulse energy over an extended time window and reducing the overall net peak intensity. At the output of the fiber, these linearly chirped pulses can be compressed using an appropriately dispersive element such as a bulk grating pair or a prism-based dispersive delay line. Compression factors of 10–20 are quite usual. Using this technique, pulse energies approaching 1 μJ have been achieved at a wavelength of $\sim 1.06 \mu\text{m}$ using relatively conventional Yb³⁺-doped LMA fiber amplifiers [92,93], and pulse energies approaching 10 μJ (peak powers $> 50 \text{ MW}$) should ultimately be possible using state-of-the-art fibers.

(b) *Fiber-based CPA*: The well-known technique of CPA [94] can also be applied to fiber-based laser and amplification systems [95–97]. In CPA, the short pulses to be amplified are stretched in time (say from 100 fs and typically up to $\sim 1 \text{ ns}$) using a highly dispersive element. These stretched pulses can then be amplified to high energy without generating excessive SPM within the fiber amplifiers, since the peak power is reduced in proportion to the stretching ratio employed. These high-energy pulses can then be recompressed back to their starting duration, and thus very high peak intensities can be achieved. There are various options as to the components to be used for both stretching and compressing the short pulses. To stretch the pulses, one can use a length of dispersive single-mode fiber, a bulk grating compressor, or more recently chirped fiber Bragg gratings (providing a very com-

compact and attractive option). To compress the high-energy pulses at the amplifier output, where the peak power is much higher, a bulk grating compressor is normally used, although again the use of fiber or volume Bragg gratings (VBGs) or, more recently, hollow-core photonic bandgap fibers (PBGFs) has been reported [98]. Using bulk grating compressors and LMA fiber amplifiers, femtosecond pulses with energies in excess of 1 mJ have been obtained [96], although pulse energies of $\sim 100 \mu\text{J}$ are more reliably achieved. The maximum pulse peak powers reported from fiber CPA systems have now exceeded 1 GW [97], and 10 GW is not an unrealistic target with state-of-the-art fibers and improved stretchers and compressors. It is worth adding that since the spatial mode quality achievable with fiber amplifier systems is so good, it is possible to focus beams from fiber CPA systems down to extremely tight dimensions, of say just a few μm^2 , meaning that field intensities of order 10^{16} – 10^{17} W/cm^2 should ultimately be achievable.

4. HIGH POWER FIBER LASERS AT OTHER WAVELENGTHS

For the many reasons already discussed Yb continues to be the frontrunner for high power fiber lasers. Nevertheless, although broad, the emission is restricted to the ~ 1 – $1.2 \mu\text{m}$ wavelength band, limiting the number of applications. Although inferior to YDFLs in certain respects, silica fibers doped with other RE ions also offer a route to high average power levels in a number of other wavelength bands in the near infrared spectral regime around $0.9 \mu\text{m}$ out to the short-wavelength mid-infrared regime around $2.1 \mu\text{m}$. See, for example, [99] for a survey of the wavelength coverage of different high power fiber lasers. Most of the attention has so far focused on cladding-pumped Er- and Tm-doped silica fibers which provide emission wavelengths in the ~ 1.5 and $\sim 2 \mu\text{m}$ bands, respectively. Both laser schemes have been scaled to output power levels in the hundred-watt regime and beyond, but power scaling is much more challenging than for YDFLs, so the maximum output powers achieved to date are some way behind those demonstrated for Yb fiber lasers. Nevertheless, Er- and Tm-doped silica fiber lasers have enormous power-scaling potential in wavelength regimes where there is a wealth of applications. In this section, we briefly review the current state of the art for high power Er and Tm fiber lasers, the main challenges for further power scaling, and future prospects. We also briefly review progress in power scaling of some of the other popular laser transitions in fiber gain media.

A. Er-Doped Fibers at 1.5–1.6 μm

Er-doped silica fibers provide a route to high power in the ~ 1.5 – $1.6 \mu\text{m}$ wavelength region corresponding to the $^4I_{13/2}$ – $^4I_{15/2}$ transition. In cladding-pumped configurations, it has become a standard practice to use a phosphosilicate core composition with ytterbium added to the core as a sensitizer [27,28,99]. Pump light is absorbed by the Yb^{3+} ions, and the Er^{3+} ions are subsequently excited indirectly by energy transfer from the Yb^{3+} ions (see Fig. 7). This allows pumping by high power diode lasers in the 910–980 nm band, relaxing the demands on the pump wavelength compared to unsensitized Er-doped fibers

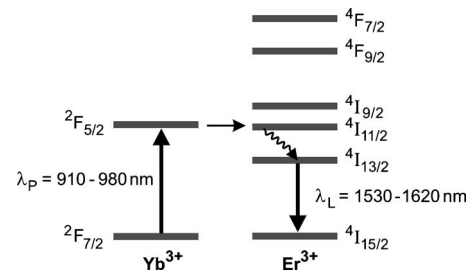


Fig. 7. Energy level diagram for Er,Yb co-doped silica.

and, via the use of relatively high Yb^{3+} ion concentrations, yields a much higher pump absorption coefficient, as required in cladding-pumped fiber configurations with a small core-to-cladding area ratio. The use of a high Yb^{3+} ion concentration in combination with a phosphosilicate host also helps to ensure efficient energy transfer from Yb^{3+} to Er^{3+} [100], which is essential for operation at high power levels. Cladding-pumped Er,Yb co-doped fiber lasers can be designed to operate at any wavelength in the band ~ 1530 to $\sim 1620 \text{ nm}$ [101,102], but operation at the short-wavelength end of this band is considerably more challenging in terms of the demands placed on fiber design, pump wavelength, and pump brightness. The maximum cw power reported to date for a cladding-pumped Er,Yb co-doped fiber laser is 297 W at 1567 nm [103]. This laser employed a simple resonator configuration comprising a 6 m long Er,Yb co-doped double-clad fiber with a $30 \mu\text{m}$ diameter (0.21 NA) core and a $600 \mu\text{m}$ diameter D-shaped silica inner cladding. Feedback for lasing was provided by a perpendicularly cleaved fiber facet and by a butted high reflectivity mirror. The fiber was pumped by a diode-stack at $\sim 975 \text{ nm}$ and yielded 297 W of output at 1567 nm in a beam with an M^2 parameter of 3.9 for $\sim 1.3 \text{ kW}$ of pump. 100 W class single-mode linearly polarized all-fiber sources [104] and wavelength-tunable erbium fiber sources [105] have also been reported.

The Stokes efficiency, and hence the upper limit on the slope efficiency for this transition, is $\sim 62\%$. However, slope efficiencies for cladding-pumped Er,Yb fiber lasers are typically in the range $\sim 40\%$ – 45% at best and at high pump powers can be much lower due to parasitic emission (ASE or lasing) on the Yb transition at $\sim 1 \mu\text{m}$ (e.g., [103]). Indeed, self-pulsed lasing at $\sim 1 \mu\text{m}$ is a common cause of damage to the fiber end facets or pump diodes in high power Er,Yb fiber lasers and amplifiers. The use of a carefully optimized core design with host composition and Er and Yb ion concentrations selected to enhance the energy-transfer efficiency and raise the threshold for parasitic emission at $\sim 1 \mu\text{m}$ is crucial for power scaling and makes fabrication of Er,Yb co-doped double-clad fibers more challenging than for simpler (singly doped) fibers. Additional precautions, such as the use of appropriate dichroic mirrors to protect pump diodes, can also help to reduce the risk of damage. Also, operation at elevated temperatures increases the threshold for Yb parasitic lasing (due to the increased three-level character) and can also be used to increase the Er lasing efficiency [106].

B. Thermal Limits

While it is certainly true that fiber lasers enjoy a degree of natural immunity from the effects of heat generation

(by virtue of their geometry), they are not completely immune. Indeed, the onset of thermally induced damage or degradation to the fiber's outer-coating is one of the main factors limiting the average output power from cladding-pumped Er,Yb fiber sources. In most designs of double-clad fiber, the outer-coating serves both as a protective layer and as the low-index layer allowing pump light to be guided in the inner-cladding pump guide. Usually, the outer-coating is a low refractive index fluorinated polymer that can withstand temperatures up to $\sim 150^\circ\text{C}$ – 200°C before the onset of damage, and 80°C has been suggested as the limit for long-term reliability [107]. The upper limit on heat deposition density in the core, $P_{h\text{ max}}$, that can be tolerated before the onset of coating damage can be estimated from [108]

$$P_{h\text{ max}} \approx 4\pi(T_d - T_s) \left[\frac{2}{K_{oc}} \log_e \left(\frac{r_{oc}}{r_{ic}} \right) + \frac{2}{r_{oc}h} \right]^{-1}, \quad (5)$$

where T_d is the maximum temperature that the coating can tolerate, T_s is the temperature of the surroundings (or heat-sink), K_{oc} is the thermal conductivity of the outer cladding (i.e., the coating), r_{oc} is the radius of the outer cladding, r_{ic} is the radius of the inner cladding, and h is the heat transfer coefficient. In situations where convective cooling is the predominant cooling mechanism, as is frequently the case in fiber lasers, the second term in square brackets of Eq. (5) dominates favoring the use of larger diameter fibers for power scaling as in [103]. Figure 8 shows the maximum heat deposition density as a function of the heat transfer coefficient (h) for a typical cladding-pumped fiber source with $r_{ic}=200\ \mu\text{m}$, $r_{oc}=250\ \mu\text{m}$, and $K_{oc}=0.1\ \text{W m}^{-1}\ \text{K}^{-1}$. It can be seen that $P_{h\text{ max}}$ is strongly dependent on the heat transfer coefficient and hence on the heat-sinking configuration. If we assume that quantum defect heating provides the sole contribution to heating, then the theoretical upper limit on output power $P_{L\text{ max}}$ for a given single-end-pumped fiber laser or amplifier before the coating damage limit is reached can be estimated from

$$P_{L\text{ max}} \approx \frac{P_{h\text{ max}} \eta_{\text{abs}}}{\alpha_p} \left(\frac{\eta_q \nu_L}{\nu_p - \eta_q \nu_L} \right), \quad (6)$$

where ν_L is the lasing frequency, ν_p is the pump frequency, α_p is the absorption coefficient for pump light launched into the inner cladding, η_{abs} is the fraction of pump light absorbed in the fiber, and η_q is the pumping quantum efficiency (i.e., the number of excited ions in the

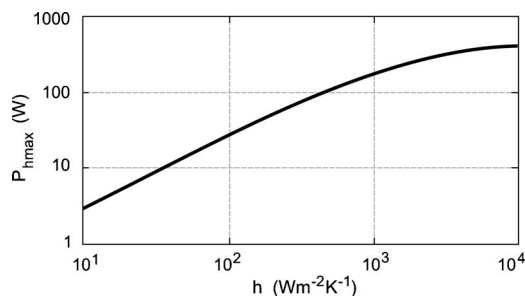


Fig. 8. Maximum heat deposition density ($P_{h\text{ max}}$) before the onset of coating damage as a function of heat transfer coefficient (h).

upper laser level manifold for each pump photon absorbed. Hence for a typical cladding-pumped Er,Yb fiber laser with an effective pump absorption coefficient of $0.92\ \text{m}^{-1}$ (i.e., $4\ \text{dB m}^{-1}$), the heat transfer coefficient would need to exceed $300\ \text{W m}^{-2}\ \text{K}^{-1}$ to allow thermal-damage-free operation at the $100\ \text{W}$ power level for the fiber design above. It is worth noting that an equivalent Yb fiber laser operating at $1080\ \text{nm}$ and cladding-pumped by a diode source at $975\ \text{nm}$ could generate over $0.55\ \text{kW}$ before the onset of thermal damage. Thus, effective thermal management is crucial for power scaling of Er,Yb fiber lasers, and heat generation is currently one of the main factors limiting output power.

C. Yb-Free Er-Doped Fibers In-band-Pumped at $1.5\ \mu\text{m}$

An alternative strategy for power-scaling Er fiber lasers is to pump directly into the upper manifold using a pump wavelength in the ~ 1.45 – $1.53\ \mu\text{m}$ wavelength region. This has the attraction that the need for Yb co-doping is avoided along with the problems (e.g., ASE, parasitic lasing, self-pulsing, and even damage) that can arise due to incomplete energy transfer from Yb to Er, resulting in a buildup of excited Yb ions. These problems become more pronounced at the high Er excitation densities required for the generation of high-energy pulses. Another attraction of this approach is that thermal loading due to quantum defect heating in the Er fiber is dramatically reduced from $\sim 40\%$ to a few percent. High power diode lasers at the relevant pump wavelengths are now commercially available from an increasing number of vendors. Their optical efficiencies ($\sim 35\%$) and output powers are somewhat lower than for pump diodes in the 900 – $980\ \text{nm}$ regime, but this is partly offset by the lower quantum defect pumping cycle. Recent work by Dubinskii *et al.* [109] demonstrated an Yb-free Er-doped silica fiber laser with $\sim 48\ \text{W}$ of output at $1590\ \text{nm}$ cladding-pumped by six fiber-coupled InGaAsP/InP line-narrowed LD modules at $1532.5\ \text{nm}$. The optical-to-optical efficiency was $\sim 57\%$ with respect to absorbed pump power. This is far below the quantum limit, but is nevertheless much higher than the optical-to-optical efficiencies achieved in cladding-pumped Er,Yb co-doped fibers. Further optimization of Yb-free Er-doped silica fibers tailored for high power cladding-pumped laser configurations in combination with advances in InGaAsP/InP diode laser technology to increase power, brightness, and efficiency (all currently much below the values of $9xx\ \text{nm}$ diodes) is likely to yield a significant improvement in Er fiber laser performance, particularly so because the low pump absorption of Er calls for high-brightness pumping. This also makes tandem-pumping an attractive option. For example, Nicholson *et al.* reported a HOM erbium-doped fiber amplifier pumped by a single-mode fiber Raman laser at $1480\ \text{nm}$ [110]. At $34\ \text{W}$ of pump power, this produced $10.7\ \text{W}$ of average output power at $1554\ \text{nm}$ in $100\ \text{kHz}$ $1\ \text{ns}$ pulses. Thus, Er fiber lasers may eventually be able to challenge the supremacy of YDFLs in terms of output power.

D. Tm- and Ho-Doped Fiber Lasers at $2\ \mu\text{m}$

Tm-doped silica fiber lasers also offer a route to very high output power. A particularly attractive feature of Tm-

doped silica is the very broad emission spectrum for the ${}^3F_4\text{-}{}^3H_6$ transition, spanning the wavelength range from ~ 1700 to ~ 2100 nm [111]. This provides wide flexibility in operating wavelength and serves as an excellent starting point for nonlinear frequency conversion to the mid-infrared. A further attraction of Tm-doped fibers is the ability to scale to much larger mode areas than for Yb-doped fibers while maintaining single-mode operation, by virtue of the longer operating wavelength. This opens up the possibility of levels of performance in cw and pulsed modes of operation beyond the capabilities of Yb-doped fiber sources by virtue of the ability to raise the threshold for unwanted nonlinear loss processes (SBS and SRS) and catastrophic damage.

Tm-doped silica has three main absorption bands relevant to high power operation (see Figs. 9 and 10). The two most attractive absorption bands are at $\sim 780\text{--}810$ nm and at $\sim 1550\text{--}1750$ nm. The latter pump band coincides with the emission wavelengths available from cladding-pumped Er fiber sources, thus allowing very low quantum defect (in-band) pumping and very high slope efficiencies (70%–80%) to be achieved [112], comparable to those demonstrated in YDFLs. A further attraction of this pumping scheme is the high brightness of the Er fiber pump laser, which allows the use of core-pumped Tm fiber laser configurations or high core-to-cladding area ratio Tm fiber lasers, giving flexibility in core design and doping levels as well as access to lasing wavelengths (~ 1725 to ~ 2100 nm) across most of the emission band [112]. Meleshkevich *et al.* reported a Tm-doped silica fiber laser cladding-pumped by multiple Er fiber lasers with 415 W of single-mode output at 1940 nm limited by the available pump power [113].

The absorption band at 780–800 nm can be pumped with commercial high power diode lasers. This has the attraction of simplicity compared to the former approach, but more conventional double-clad fiber designs are required due to the lower brightness of the diode pump sources. Hence the lasing wavelength is generally restricted to longer wavelengths in the range $\sim 1850\text{--}2100$ nm. The Stokes efficiency for this pumping scheme is relatively low, ~ 0.4 , implying a rather low efficiency. However, the efficiency can be improved dramatically by exploiting the “two-for-one” cross-relaxation process (${}^3H_4+{}^3H_6\rightarrow{}^3F_4+{}^3F_4$) [114]. While this has become a standard approach for improving the efficiency in diode-pumped Tm-doped crystal lasers for over two decades [114], the first demonstration of a cladding-pumped Tm-doped silica fiber with efficiency enhanced by cross-relaxation was only 10 years ago [115]. In this work, the

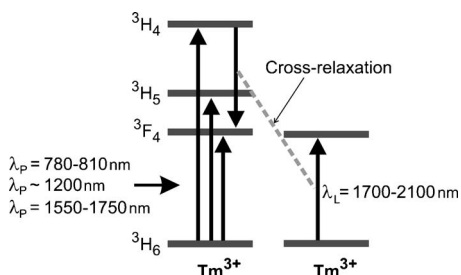


Fig. 9. Energy level diagram for Tm-doped silica.

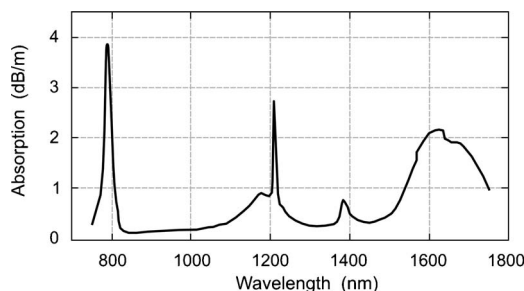


Fig. 10. Absorption spectrum for Tm-doped silica.

fiber laser yielded a maximum output power of 14 W at ~ 2 μm for 36.5 W of diode pump power at 787 nm using a Tm-doped aluminosilicate double-clad fiber with a Tm concentration of $\sim 1.4\%$ (by weight). Since then dramatic improvements in the efficiency for cladding-pumped Tm fiber lasers have been achieved by modifying the core composition and Tm doping level to promote the two-for-one cross-relaxation process while limiting the detrimental impact of other spectroscopic processes (notably energy-transfer upconversion) on performance [116]. The optimum Tm doping level depends on the mode of operation and desired operating wavelength, but is generally considered to be around 3% (by weight) for most cw laser configurations operating toward the long-wavelength end of the emission spectrum [117]. The record slope efficiency with respect to the absorbed pump power reported for a Tm-doped silica fiber laser cladding-pumped at ~ 0.8 μm is 74% [116], which compares favorably with the efficiencies routinely achieved with cladding-pumped Yb fiber lasers. In practice for higher power Tm fiber lasers based on commercially available fibers, slope efficiencies are somewhat lower ($\sim 60\%$), but still well above the Stokes efficiency. If we assume for a typical high-Tm-concentration silica fiber laser that the pumping quantum efficiency is $\sim 1.7\text{--}1.8$, then from Eq. (5) the upper limit on output power before the onset of coating damage is around four times lower than for an equivalent YDFL. Clearly, high-Tm-concentration large-core double-clad fibers have huge advantages in terms of the ability to mitigate unwanted nonlinear processes and catastrophic damage, but effective thermal management is crucial for scaling to very high power levels. Moulton *et al.* recently reported a double-clad Tm-doped silica fiber laser with 885 W of output at ~ 2040 nm in a MM beam with M^2 parameters of 6 and 10 in orthogonal planes [117]. Pump light was provided by two 1 kW fiber-coupled diode pump modules at ~ 797 nm. Ehrenreich and co-workers recently demonstrated an “all-glass” Tm fiber MOPA based on a 50 W Tm fiber oscillator at 2045 nm and two Tm fiber power amplification stages with over 1 kW output power and with a slope efficiency of $\sim 53\%$ [118]. This result represents the highest output power reported to date for a Tm fiber source and serves as a very convincing demonstration of their power-scaling potential in the 2 μm wavelength regime. The combination of power scalability and wide wavelength flexibility is a very useful feature and should open up the prospect of many new applications.

Cladding-pumped Tm fibers have also been deployed in more sophisticated MOPA architectures to yield wavelength-tunable and narrow-linewidth output at

power levels in the hundred-watt regime and above. Pearson and co-workers recently reported a linearly polarized single-frequency Tm fiber MOPA based on a single-frequency Tm fiber distributed feedback (DFB) master oscillator followed by three Tm fiber amplifier stages with 100 W of output at 1943 nm [119]. Goodno and co-workers reported a single-frequency MOPA based on a DFB diode laser and four Tm fiber amplifiers with a non-PM (i.e., non-polarization-maintaining) cladding-pumped final amplifier that produced 608 W of output [120].

This serves once again to underline the potential of Tm fiber sources. It is worth pointing out that while the popular trend for power-scaling Tm fiber sources has been to exploit the two-for-one cross-relaxation process using commercial diode pump sources at $\sim 0.8 \mu\text{m}$, this is not the route that ultimately offers the highest power levels. If efficiency, cost, and complexity considerations are put aside, then in-band pumping with multiple high power Er fiber lasers almost certainly offers the prospect of higher output power with greater flexibility in operating wavelength and mode of operation. Thus, with forthcoming advances in fiber component technology for the $2 \mu\text{m}$ wavelength regime, we are likely to see further significant improvements in performance for Tm fiber-based sources.

Extension to wavelengths a little beyond $2.1 \mu\text{m}$ (limited by material and impurity absorption) can be achieved using a Ho-doped silica fiber laser operating on the $^5I_7\text{-}^5I_8$ transition [121]. Ho-doped silica offers a very broad emission line extending beyond $2.1 \mu\text{m}$ and can be pumped directly at $\sim 2 \mu\text{m}$ using a diode laser or a high power Tm fiber laser [121] or, indirectly, via co-doping with Tm^{3+} followed by energy transfer from Tm^{3+} to Ho^{3+} [122]. In the latter approach, the Tm^{3+} ions can be excited using any of the pumping schemes described above, and thus Ho fiber lasers should be scalable to very high power, complementing the wavelength band offered by Tm fiber lasers.

5. FUTURE PERSPECTIVES

As the previous sections have shown progress in all areas of fiber laser technology over the past 15 years or so has been staggering with an increase in the average output power in excess of 60% year on year even in mature areas, and with much faster growth for less mature devices. From the perspective of the raw generation of power it is clear from the preceding discussions that the fundamental average power limits for single transverse mode operation are within sight, and that without major new breakthroughs in mode area scaling/mode control within MM fibers and improved thermal and damage management, the record output powers will saturate at the ten to several tens of kilowatts level from a single core. Likewise, with regard to pulsed operation again we are relatively close to achieving the maximum peak power that might be achieved from a single core at $1 \mu\text{m}$ —improved peak powers approaching one order of magnitude higher might be achieved by extending existing pulsed technology to longer wavelengths and taking benefit from the reduced nonlinear effects due to the increased core sizes possible; however substantial improvements in the peak power will only be achieved by new concepts for further mode area scaling and by the use of substantially shorter device

lengths to reduce the impact of fiber nonlinearity. However that brings forth the conflict between the requirements for a short fiber for nonlinear mitigation and a long fiber for thermal management. The self-focusing limit that depends simply on power within the fiber, and therefore cannot be addressed by a larger mode area, is also now within sight and will need to be considered much more moving forward. Once the single-aperture limits are truly reached, then beam combination will be the only route available to extend both cw and pulsed performance.

Given these conclusions we next consider the technical advances that need to be pursued to underpin the next decade of sustained growth in fiber laser performance—in particular in terms of brighter pump sources for fiber lasers, improved power handling (both thermal and optical powers), extended wavelength coverage, and improved beam combination technology. It is to be appreciated that the technological improvements we anticipate can also be used to provide increased options in terms of source control, improved reliability, and flexibility in system design, which from a commercial perspective is arguably often far more important than improved headline laboratory performance metrics and can result in significant cost savings and new market opportunities. Obviously, such benefits are often hard to substantiate and to quantify.

A. Improved Pump Sources and Pumping Options

1. Higher-Brightness Diode Pump Sources

When considering the future prospects for cladding-pumped fiber lasers, it is worth noting that the dramatic advances in high power fiber laser technology did not follow immediately after the invention of the LD-pumped double-clad fiber by Kafka in 1989 [24]. Indeed the first demonstration of a 100 W Yb fiber laser was over a decade later [32]. In truth, as with so many inventions, the cladding-pumped fiber laser was born before its time in the sense that diode pump sources with sufficient output power and brightness were not yet available. In contrast to the situation for most bulk solid-state laser architectures, the requirement for raw pump power must be accompanied by high pump beam brightness to allow efficient coupling into the fiber. Thus, in many respects, the dramatic rise in power and performance attainable from fiber lasers has mirrored developments in diode pump sources in terms of output power and, in particular, brightness. This is likely to remain an underpinning theme also in the future, despite the emergence of tandem-pumping as an increasingly attractive option for high-brightness pumping. To get a sense of what the future holds, it is worth quickly reviewing the state of the art in terms of diode pump sources and possible future developments over the next decade to see how these could benefit fiber laser technology.

A number of different diode pump sources have been employed to power scale fiber lasers. Diode-bars and stacks offer the attraction of high power-to-package volume, but yield rather low brightness (primarily because of their low fill-factors), and hence require somewhat complicated free-space optical arrangements to produce output beams compatible with the requirements for cladding-

pumping of fibers. A further drawback of these pump sources is that rather aggressive cooling is needed to cope with the high thermal loading density. Alternatively, broad-area (MM) single emitters offer high reliability, simple thermal management, and the highest brightness per unit emitter area with output power levels up to ~ 10 W from ~ 90 – 100 μm wide emitters in the ~ 915 – 975 nm band. Fiber-based aggregation schemes employing multiple fiber-coupled broad-area emitters (see Fig. 11) in conjunction with MM fiber combiners [123] allow robust scaling of pump power. Not surprisingly, this pumping architecture has become the architecture of choice for many in the field and is at the heart of many industrial high power fiber laser products. One of the main drawbacks of this approach is that the diode emitter brightness is degraded by more than one order of magnitude on launching into the MM delivery fiber. This is largely because the M^2 parameter parallel to the diode junction (M_x^2) is typically ~ 15 – 20 times larger than for the orthogonal direction, and hence the delivery fiber's core size and NA must be selected to accommodate the slow-axis beam size and divergence.

This shortcoming can be remedied by reducing the slow-axis divergence of the diodes. This is attractive because the package architecture remains unaltered. While it is proved difficult to reduce the emitter size because of limits on the power density on the facet and the fiber diameter because of handling issues of very thin fibers, there has been good progress in the reduction of diode NA. Thus, whereas the fiber pigtailed support a NA of 0.22, it is now possible to get pigtailed diodes working at NAs of less than 0.12 [124]. A more radical approach is to use a spatially combined multi-emitter architecture. One example of such a scheme is illustrated schematically in Fig. 12. In this approach the individual emitters are collimated in the fast-direction by cylindrical microlenses and then spatially combined using a simple arrangement of mirrors prior to being coupled into the delivery fiber. Successful implementation of multi-emitter sources requires careful design and construction since the tolerance on position of optical components is much more demanding than for fiber-coupled single emitters. However, this approach, in combination with polarization combining, can yield a 10- to 20-fold increase in power and brightness per delivery fiber.

Further increases in power and brightness can be achieved via the use of wavelength beam combining [125]. One can envisage a spatially combined multi-emitter source (similar to the configuration shown in Fig. 12) employing VBGs in an external feedback cavity arrangement to select the same operating wavelength of all emitters within a narrow band (say <0.5 nm). Then multiple multi-emitter sources (each with a different operating wavelength) could be combined into a single beam using

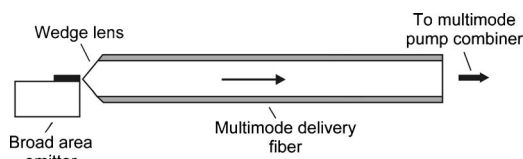


Fig. 11. Fiber-coupled broad-area pump diode.

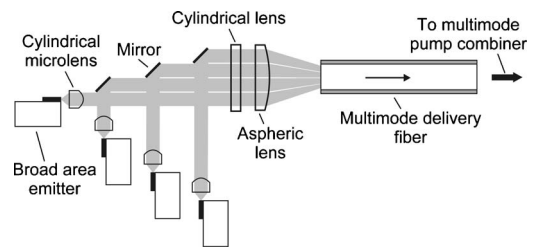


Fig. 12. Spatially combined multi-emitter diode pump source.

an arrangement of VBGs [126]. The theoretical upper limit on the number of multi-emitter sources that could be combined in this way depends on their linewidths and on the useful absorption bandwidth of the RE ion doped fiber. However, the practical upper limit on the number of combined sources is also dependent on the residual losses (i.e., due to scattering, absorption, and imperfect antireflection coatings) of the optical components. For most RE ion pump transitions it should be possible to combine at least ten multi-emitter sources into a single delivery fiber using this approach. The net result would be over two orders of magnitude increase in power and brightness compared to a fiber-coupled single-emitter to yield a total power of over 1 kW per fiber. Clearly, the construction of such a source would be very demanding on optical components and on alignment tolerances; and, thus, when these practical considerations are factored into the design, the level of performance achievable may be somewhat lower. Nevertheless, it is clear that there is enormous scope for an increase in pump power and brightness compared to what is currently available from high power diodes. This will have a huge impact on cladding-pumped fiber lasers, although it is certainly possible that tandem-pumping, which is already in commercial use and provides very high pump brightness, will also continue to be the favored approach in the future in many cases.

The maximum pump power $P_{p \max}$ that can be launched, via a single injection point, into a double-clad fiber using the present generation of broad-area emitter pump diodes in conjunction with the various beam combination schemes described above and MM fiber combiner aggregation schemes can be estimated from

$$P_{p \max} \approx \frac{2P_s N \eta_{\text{coupling}}}{M_x^2 M_y^2} \left(\frac{\pi r_{ic} \theta_{\text{NA}} \gamma}{\lambda_p} \right)^2, \quad (7)$$

where P_s is the power available from a constituent single-emitter diode, M_x^2 and M_y^2 are the beam propagation factors for the single-emitter diode after fast-axis collimation, N is the number of wavelength-combined multi-emitter sources, η_{coupling} is the coupling efficiency through the pump beam conditioning and combining optics and into the active fiber, θ_{NA} is the arcsine (NA), γ is a factor (<1) to account for the need to slightly underfill the fiber's aperture and NA to avoid damage to the outer-coating and mounting components, and λ_p is the pump wavelength. Figure 13 shows the theoretical upper limit on the launched pump power as a function of the inner-cladding diameter based on current power levels available from ~ 100 μm wide broad-area emitters in the 915–975 nm band (i.e., $P_s = 10$ W), and assuming $\theta_{\text{NA}} = 0.4$, $\eta_{\text{coupling}} = 0.8$, and $\gamma = 0.8$. Three different scenarios are

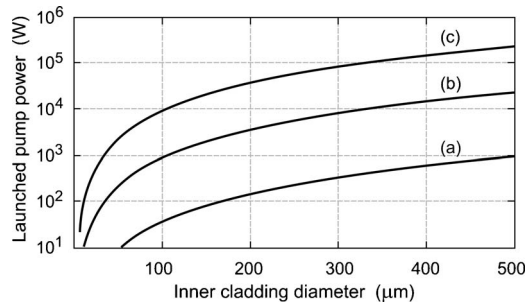


Fig. 13. Theoretical limit on launched pump power for broad-area emitter-based pump schemes assuming $P_s=10$ W, $\theta_{NA}=0.4$, $\eta_{\text{coupling}}=0.8$, and $\gamma=0.8$. The curves show the upper limit on launched power that can be achieved using (a) fiber-coupled broad-area emitters, (b) spatially combined and polarization-combined multi-emitter sources, and (c) ten wavelength-combined multi-emitter sources.

considered. Curve (a) shows the upper limit on the launched power that can be achieved using fiber-coupled single emitters. Curve (b) shows the upper limit on the launched power using spatially combined and polarization-combined multi-emitter sources. Curve (c) shows the upper limit on the launched power for a wavelength-combined multi-emitter source with $N=10$. Thus, using the current single-emitter diode technology in combination with spatial, polarization, and wavelength beam combination could yield launched pump powers that are two orders of magnitude higher than can routinely be achieved today for a given inner-cladding diameter and NA. In practice, the pump power that can be accommodated by a given fiber will also depend on thermal damage limits for optical components, MM fiber combiners, delivery fibers, and the final active fiber. Thus, the development of “next generation” high-brightness diode pump sources will be very challenging.

2. High-Brightness Tandem-Pumping

There are several attractions of tandem-pumping, and one of them is the high pump brightness. This exceeds that of even the brightest diode pump sources envisaged in the future by at least 2 orders of magnitude. A more complex system, a lower overall efficiency, and a limited range of pump wavelengths may appear to be disadvantages of tandem-pumping, as compared to direct diode-pumping. However, if we consider high-brightness diode-based pump sources, these are in themselves sophisticated systems (see Fig. 12) that may well be as complex as a fiber-laser pump source. The chips used for high-brightness diodes are also somewhat less efficient than those of lower-brightness diodes, and spectral beam combination introduces losses, too. Therefore, all told, in the high-brightness pumping regime, tandem-pumping with a simple intermediate fiber pump laser can perhaps be more efficient than direct diode-pumping, in some cases. Furthermore, the possibility of Raman shifting greatly extends the wavelength coverage of tandem-pumping. This can benefit several RE ion laser transitions, which are currently more severely affected than Yb-doped fibers by the low brightness of pump diodes at appropriate wavelengths. For example, a Raman-shifted YDFL providing 73 W at 1480 nm was recently used to

core-pump an erbium-doped fiber on a single HOM [110]. However, except for core-pumping, it will be challenging to maintain the high brightness in the final gain fiber, i.e., launch and guide the pump in a small inner cladding. This may not be strictly necessary, but improves the pump overlap with the core, which shortens the absorption length. Therefore, to make the most of tandem-pumping, it is necessary to optimize the fiber designs and pump launch schemes.

3. Summary of Likely System Benefits

The benefits in terms of fiber laser performance to be derived from improved pump sources depend very much on the situation. One obvious benefit is the ability to scale to higher average output powers in both cw and pulsed modes of operation, and we remind ourselves that some operating regimes and some wavelengths demand particularly high pump brightness. On the other hand, this is subject to limitations imposed by damage and nonlinearity, and it is already now possible to design lasers that reach the damage threshold even operating cw. For those, the benefits of higher pump brightness are less clear. Nevertheless, higher pump brightness will also relax the constraints on the core composition in many cases, allowing the use of much lower RE ion concentrations with enhanced resistance to photodarkening [127] and reduced unwanted spectroscopic loss processes (e.g., energy-transfer upconversion). This will in turn allow much easier tailoring of the refractive index profile and RE ion doping profile to facilitate robust single-mode operation in a LMA core design, which is important to mitigate both nonlinear degradation and damage. Thus, in many respects, pump brightness is still the key to further power scaling. The availability of much higher power and much higher brightness pump sources will almost certainly change current thinking on cladding-pumped fiber designs, opening up many new possibilities and yielding significantly improved performance in all operating regimes. These developments will further underline the important future role to be played by fibers in the high power laser arena.

The ability to use much smaller inner-cladding sizes for a given pump power (by virtue of the higher pump brightness) will allow the use of much shorter fiber lengths, raising the threshold for unwanted nonlinear processes (e.g., SBS and SRS). This will benefit fiber sources (e.g., narrow-linewidth and pulsed) where the upper limit on power is determined by the onset on nonlinear processes, opening up the possibility of a dramatic increase in power. At some point, however, the increased thermal loading density will become a problem, as will be discussed below, but we reiterate that high-brightness tandem-pumping can be beneficial also in reducing the total thermal load in the gain fiber.

B. Improved Power Handling

1. Improved Thermal Management

Although increased pump brightness brings many direct and indirect advantages to many devices, the use of shorter fibers with higher thermal loading densities will emphasize the need to improve thermal management.

Power-extraction per unit length can exceed 1 kW/m [128] in YDFs, but aggressive cooling is required to avoid damage. With conventional double-clad fibers with a low-index polymer coating, the coating is often most sensitive to a high thermal load. Other thermal effects are normally less of a problem [129]. The coating serves the dual purpose of guiding the pump light and protecting the fiber, and this restricts the materials and designs available. Silicone has been used in the past. It can withstand higher temperatures, but suffers from degradation over time, and the resulting pump NA has been restricted to around 0.4. Teflon (polytetrafluoroethylene) is an interesting high-temperature high-NA option. However it is expensive and difficult to apply, and although Teflon coatings are commercially available for passive fibers (e.g., [130]), the benefits for high power fiber lasers have yet to be demonstrated.

Today's preferred low-index coatings (fluorinated acrylates), while easily applied during fiber drawing and possessing excellent optical properties, are relatively poor from a thermal point of view. They degrade quickly at temperatures approaching 200°C and long-term reliability may require operation below 80°C [107]. Furthermore, their thermal conductivities are poor, e.g., around $0.24 \text{ W K}^{-1} \text{ m}^{-1}$ [107]. Therefore, if special attention is paid to achieving a high heat transfer coefficient h , the first term in Eq. (5) will dominate, and the highest temperature reached within the coating, at the interface with the silica inner cladding, is largely determined by its own thermal impedance. The temperature difference across the coating depends on the inner-cladding diameter and coating thickness. The use of thin coatings will result in a fiber with improved thermal resilience. The challenge for the future lies in realizing a thin coating within the constraints of providing good optical guidance. We have fabricated fibers with coating thicknesses of 20 μm , with a reduction in the thermal impedance of nearly a factor of 5 compared to a more conventional coating thickness of 100 μm .

The temperature difference from the ambient to the outside of the coating can be substantial, too, and is likely to dominate the temperature rise seen by the inside of the coating in the case of unforced air-cooling, for example. More efficient heat transfer arrangements are needed in many cases, ranging from straightforward measures such as coiling the fiber on a metal heat-sink to immersing it in water, which presents practical problems and long-term reliability issues. It is also possible to embed the fiber in a metal. This can drastically reduce the overall thermal impedance through a conventional heat-sink (cold-plate, water-cooled heat-sink, etc.), although the different melting points and thermal properties of the many different types of materials involved make this a nontrivial proposition. In the example of Fig. 8 above, a heat transfer coefficient of $10^4 \text{ W m}^{-2} \text{ K}^{-1}$ would be sufficient to make the temperature difference between the outside of the coating and the ambient negligible, but a higher value is required for a thinner coating.

Thermal management becomes simpler if the requirements on the polymer coating are relaxed. In so-called all-glass structures, the waveguides are defined entirely by a glass. No light reaches the coating (if the scatter is negli-

gible), so the coating material can be selected to aid thermal management rather than for pump guiding. This opens up opportunities for protective coatings made of thin high-temperature polymers as well as metals. The jacketed air-clad fiber [20,131] is one type of all-glass fiber that can provide NAs of 0.7 [132] and above, but the silica:air mesh that constitutes the low-index outer cladding also serves as an insulating layer. This increases the temperature in the glass, which is normally not critical, but nevertheless undesirable. Furthermore, the thermally induced stresses in the mesh can be substantial [133] and can conceivably break it. To date, this type of fiber has been limited to 2.5 kW of output power [134].

Instead of a silica:air mesh, a low-index glass can be used for the outer cladding. This improves the thermal and mechanical properties, but the achievable inner-cladding NA is substantially lower than that provided by low-index polymers, so less pump power can be coupled into the fiber. This drawback can be offset by using higher-brightness pump sources to increase the launched pump power albeit at the expense of increased complexity. It is likely that the next generation of high-brightness pump sources will make all-glass fibers the natural choice for power scaling, given the benefits to be gained in terms of thermal and mechanical properties and ease of splicing compared to jacketed air-clad fibers.

In addition to the above techniques thermal problems can also be reduced by decreasing the thermal loading density by in-band pumping. This is a key strength of tandem-pumping, which has already proved to be a powerful technique for power scaling of YDFs. For example, IPG's 10 kW fiber laser was pumped by YDFs at 1018 nm and emitted at 1070 nm [14], corresponding to a quantum defect of less than 5% in the final gain stage, which is roughly half of that of a directly diode-pumped YDFL. This result serves to underline the benefits of tandem-pumping, which seems likely to remain as the option of choice for operation at very high powers.

Nonlinear scattering, rather than stimulated emission, may ultimately allow for the lowest thermal loads. For example, fiber Raman lasers, which have now been scaled beyond 100 W [135,136] and look scalable well into the kilowatt regime, can operate with quantum defects of less than 4%, in the case of silica pumped at 1060 nm. SBS can also be used for amplification, with a quantum defect of the order of 10^{-4} in silica fiber. However, high power operation presents many challenges, and powers to date have been limited. For example, an energy of 0.1 mJ was reported in the pulsed regime, in a beam clean-up experiment [137]. Finally, fiber-optic parametric amplifiers operate without any quantum-defect heating. Key challenges here are related to phase-matching, and the record power to date is only a few watts [138].

2. Improved Optical Damage Thresholds

Catastrophic optical damage due to dielectric breakdown in the core is an increasingly troublesome issue, in particular in the case of high-energy nanosecond-scale pulses. As stated earlier, the damage threshold of pulses in this regime is normally taken to be $1.5 \text{ kW ns}^{1/2}/\mu\text{m}^2$, with an inverse square-root dependence on the pulse duration [60]. Compared to thermal damage of the coating,

the options for mitigating catastrophic damage are much more limited. One option is to use materials with higher damage thresholds, but there are only few materials with higher damage thresholds than silica. On the other hand, the incorporation of REs and other typical fiber dopants is reported not to adversely affect the damage threshold significantly [139].

It is not clear if higher damage thresholds are realistic. However, some recent studies do suggest this possibility. Thus, values of around $0.5 \text{ TW/cm}^2 = 50 \text{ kW}/\mu\text{m}^2$ [140] and even $6 \text{ TW/cm}^2 = 0.6 \text{ MW}/\mu\text{m}^2$ [141] have been suggested. Given a self-focusing limit of around 4 MW at 1060 nm, and that a core area of $200 \mu\text{m}^2$ is straightforward to achieve, these values are far beyond what is needed ($\sim 20 \text{ kW}/\mu\text{m}^2$). However these damage thresholds have not been demonstrated in fibers for reasons that are partly unknown. Some reasons are readily understood, e.g., that the $0.6 \text{ MW}/\mu\text{m}^2$ can only be achieved in micrometer-sized spots [141], while larger spots lead to a lower threshold. This is attributed to propagation and self-focusing. Also the lower threshold of [140] still required carefully controlled conditions, for example, to eliminate facet reflections. Some of these conditions (e.g., a $1 \mu\text{m}^2$ spot size) are not achievable at high powers in a fiber, which clearly must allow for propagation over appreciable lengths with low nonlinear degradation.

Less clear is if material imperfections contribute to the lower damage threshold of $1.5 \text{ kW ns}^{1/2}/\mu\text{m}^2$ that is routinely seen in silica fibers. Note here that a $1 \mu\text{m}$ diameter focused spot has a volume of around $1 \mu\text{m}^3$, which is very roughly 9 orders of magnitude smaller than the core volume of a LMA fiber. Thus, it seems quite possible that a LMA fiber contains defects which lower the damage threshold and which are not readily detected with $1 \mu\text{m}^3$ samples. A better understanding may open up for higher damage thresholds, when combined with improved fabrication techniques, e.g., with higher-purity materials.

The damage threshold of $1.5 \text{ kW ns}^{1/2}/\mu\text{m}^2$ applies to bulk damage, but similar values are possible also for the surface. However, the likelihood for surface defects and impurities, e.g., from polishing compounds [140], is considerable, and this can lead to a much lower surface damage threshold. We expect the standard end-capping technique applied today to be used increasingly. This reduces the power density at the facet. One seemingly attractive option for effective end-capping is to “erase” the core at the end of the fiber by diffusion of dopants or collapsing of holes in the case of air-glass microstructured fibers. Additional benefits of end-capping include better thermal properties, reduced feedback into the guided modes, the avoidance of a high-intensity standing-wave pattern at the facet, and simpler coating of end-facets in some configurations. The deposition of anti-reflection, high-reflection, and dichroic coatings is likely to increase in the future. The benefits of this will be modest in some cases, but this is nevertheless a natural future progression.

A larger mode area is another possibility, which we will discuss further in conjunction with nonlinear degradation. We note here that even with the lower damage threshold of [60], i.e., $1.5 \text{ kW}/\mu\text{m}^2$ for 1 ns pulses, the self-focusing limit would be lower than the damage limit for mode areas above $3000 \mu\text{m}^2$. It is also worth pointing

out that the requirements on the mode distribution for nonlinearity and damage mitigation differ somewhat: for (most) nonlinearities, it is the effective area that matters, while for damage the peak modal intensity is more of a concern. It is possible to have very large effective areas, while still reaching a high peak modal intensity, e.g., in the case of a fiber operating on a HOM. Furthermore, with MM fibers, the possibility of hot spots due to modal interference is an issue, either as a transient with signals of low temporal coherence or as a more long-term effect with signals of higher temporal coherence. Mode-flattened designs can be used to reduce the peak modal intensity [142], but these do remain susceptible to modal interference.

The temporal stability of pulses is important, too. Thus, pulses with spikes (e.g., from a laser with a few longitudinal modes lasing simultaneously) have a lower damage threshold than pulses without spikes [140]. MOPAs are attractive in this regard since they can be seeded with well-controlled pulses; the desired pulse shape and control are easier to achieve with low power oscillators.

C. Improved Nonlinearity Management

Avoiding nonlinear effects in fiber is one of the most critical issues for many high power fiber laser systems. For example, SRS is a major limiting factor for current nanosecond MOPAs and will become an increasingly limiting factor in cw systems as power levels increase beyond 10 kW. SBS provides a limit to the maximum single-frequency power that can be generated in a fiber MOPA and thus will be a key issue in power scaling for coherent beam combination schemes. SPM is currently the primary limiting factor for most ultrashort pulse systems. Techniques to manage nonlinear effects either through fiber design or pulse shape control are thus essential.

1. Mode Area Scaling

As mentioned previously, increasing the effective mode area within the fiber provides the most effective way of minimizing the nonlinearity—reducing both the peak intensities and the device length due to improved pump absorption (for fixed inner-cladding dimension). Maintaining mode quality as the core area is scaled up is of primary importance, and a number of strategies to achieve this have been pursued over the years. Figure 14 illustrates various fibers relevant to this section. Initially efforts focused on increasing the core diameter while reducing the NA accordingly in order to maintain pure single-mode operation [53]. However, as the NA is lowered the guidance gets progressively weaker, meaning that light is more readily lost from the core as the fiber is bent, and this limits the minimum NA that can be used in practice to 0.04–0.05. Assuming a NA of 0.05, single-mode operation is obtained for a core diameter of up to $16 \mu\text{m}$ and a corresponding effective area of around $200 \mu\text{m}^2$ for a wavelength of $1.064 \mu\text{m}$. Using this approach a tenfold or so improvement in nonlinearity per unit length can be obtained relative to the core sizes typical of more conventional single-mode RE-doped fibers as used, for example, within telecommunications.

Larger mode areas can be achieved by relaxing the strict single-mode fiber requirements and working with

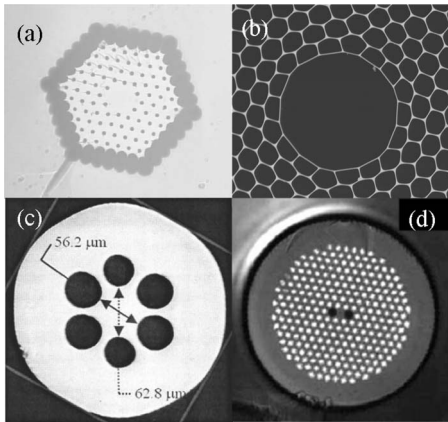


Fig. 14. Different LMA fiber designs for the mitigation of non-linearity. (a) Rod-type fiber incorporating a microstructured (air:glass) core and high-NA inner cladding [150]. (b) Air-core PBGF offering ultralow nonlinearity and high damage thresholds for beam delivery [161]. (c) Leakage channel fiber in which the leakage loss for high-order modes is arranged to be much higher than that of the fundamental [151]. (d) Solid PBGF offering PM guidance (due to stress rods placed close to the core) and in-fiber distributed spectral filtering to shape gain profiles and eliminate SRS [165].

step-index fibers at much higher V -values, such that the fiber is itself capable of supporting MM operation, but engineering the fiber device such that it operates on just a single transverse mode [143–146]. The lowest-order (LP_{01} mode) is preferred in most instances, but there is growing interest in operating on a single HOM instead [147] since these can have interesting dispersion characteristics; and, furthermore, they may be more robust to subsequent mode-coupling due to perturbations than the fundamental mode. This in turn suggests that larger mode areas can be used. A downside with the use of HOMs is that often they exhibit localized regions of high field intensity across the core that can result in problems with damage at lower values of effective area than might otherwise be expected. There is potential to avoid this by appropriate engineering of the HOM profile by control of the core refractive index profile and geometry, although little has been done to date in this area.

Single-mode operation of a MM core makes it necessary to establish means to preferentially excite, amplify, and/or attenuate specific optical modes of the fiber while at the same time ensuring that scattering between modes as the signal propagates through the amplifying fiber is minimized [143]. Much work has focused on using differential-gain by selective RE doping across the core [144,145], differential-bend-loss by controlled bending of the fiber [146], and resonant coupling of higher-order bound core modes to leaky modes (e.g., in chirally coupled core fibers [148]) to favor propagation of the fundamental mode over HOMs. Using such approaches, a further order of magnitude or so improvement in the mode area relative to the low-NA SM case can be obtained in certain circumstances. Further improvements by a factor of 5–10 may be achievable by exploiting microstructured fiber technology, in particular endlessly single-mode designs to obtain ultra-low NAs in rigid rod-type structures [149,150] (where the rigidity is required to minimize mode-coupling and/or excess bend-loss and mode distortion due to bending) or

leakage channel fibers where differential confinement or bend-loss loss can be used to favor fundamental mode operation [151]. Using these approaches mode areas in the range 5000–10,000 μm^2 at 1.06 μm have been reported in the laboratory. It is however to be appreciated that controlling the refractive index of the core in RE-doped versions of these fibers is extremely challenging. Often some form of nano-structuring of the core [89,150] is required to avoid the doped regions of the glass (which are likely to have a refractive index higher than the surrounding silica), perturbing the underlying (weak) guidance mechanism intended to provide single-mode operation. Such refractive index perturbations can severely compromise the mode area and ultimate mode quality that can be achieved. Note that most of the largest mode areas reported in the literature are for passive fibers where doping-induced refractive index perturbations, thermal stability, and transverse gain competition under saturated laser operation are not an issue. Exactly how far one can push these more exotic active fiber designs in practice will require further study and better quantification moving forward.

Another intriguing approach to LMAs worthy of mention is the use of gain guiding in an index antiguide [152], which when pumped provides optical confinement in a single gain-guided transverse mode. The basic principles have been validated, and single-mode operation in very large cores has been reported. While physically interesting, the practicality of the approach remains to be demonstrated given the very high gains per unit length needed (and the associated heat dissipation required for anything like high average power operation). Nevertheless further work in this area is worthwhile—particularly in the context of pulsed systems.

While the progress in mode area scaling appears most impressive the issue of whether the approaches providing the largest claimed mode area will ever be made practical, given the concerns of robustness, mode-stability, manufacturability, packaging, and reliability of pump coupling remain a concern. Certainly few if any commercial systems operate with fibers providing mode areas in excess of 1000 μm^2 at 1.06 μm . Significant further research into the whole area of mode scaling with a particular focus on improving practicality and high power operation is needed; however at this point it is not clear that substantial further progress will be made in terms of single-mode single-aperture emission, although clearly increased mode areas will be achievable by extending the concepts described above to longer-wavelength transitions (i.e., one might anticipate a factor of 2–4 increase moving from 1 to 2 μm).

It is however worth noting the possibility of multimode interference (MMI) operation. A tantalizing prospect of MMI devices is that they may offer a route to higher self-focusing limits in fibers with low modal dispersion, as well as larger core areas. MMI entails a large MM core that operates on several modes, but these are phased such that they interfere at the output into a free-space diffraction-limited beam or a single-mode beam of a single-mode fiber. If mode-selective feedback is arranged (e.g., when provided through a single-mode fiber), this phasing can be automatic, with the wavelength adjusting

to minimize the cavity losses and thus maximize the coupling into the single-mode fiber [153]. It is also possible to use electronic control of the modal content and phases [154], although this requires separate control for both polarizations to work well, and this has yet to be demonstrated.

Tandem-pumping appears to have an interesting role to play in mode area scaling, too. This is related to the high excitation densities and gain that can build up in regions that are not well saturated by the desired mode, and which can lead to mode instabilities and mode quality degradation in LMA fibers. Tandem-pumping helps to control the excessive excitation and gain [155] since the maximum excitation and gain are much lower when pumping close to the emission wavelength. Note here that a small inner cladding helps to reduce the absorption length in this case, so even if one can get the right wavelength with direct diode-pumping, the brightness would be inadequate for close area ratio cladding-pumping. As an example, Fig. 15(a) shows the Yb excitation level calculated across a uniformly Yb-doped phosphosilicate core for five different pump wavelengths. The fiber has a 50 μm diameter step-index core with a NA of 0.06. These are typical parameters for low-NA large-core fibers that we fabricate. This core supports 12 LP_{mn} modes at a signal wavelength of 1080 nm. The fiber is saturated by a signal at this wavelength propagating in the unperturbed fundamental mode of the fiber. Furthermore, the pump waveguide area is adjusted to yield a pump intensity that leads to an average excitation level across the signal mode of 3.0%, which is appropriate in phosphosilicate fiber for a signal wavelength of around 1070–1080 nm [156]. Thus, the gain for the signal in the fundamental mode is the same for the curves in Fig. 15(a). However, the gain for HOMs is much higher for shorter pump wavelengths due to the high excitation level at the edge of the core. Figure 15(b) shows the influence of the pump wavelength on the gain of HOMs at the signal wavelength. It also shows the highest gain of any HOM at the gain-peak wavelength, which varies with excitation level. The gain is calculated from the excitation distributions in Fig. 15(a), using a concentration of Yb ions of $2 \times 10^{26} \text{ m}^{-3}$. The gain obtained for pumps in the 910–980 nm range exceeds 6.2 dB/m for some HOMs at the gain-peak wavelength. This gain is much higher than the 0.95 dB/m we get for the saturating fundamental mode signal. Such a high gain difference is very problematic and can lead to parasitic lasing (e.g., in a catastrophic self- Q -switching mode) or otherwise self-saturation from ASE. Tandem-pumping at a longer wavelength resolves this inconsistency and facilitates further mode area scaling.

It is interesting to compare tandem-pumping close to the emission wavelength to other options for controlling the spatial gain distribution. In contrast to tandem-pumping, these are based on controlling the spatial distribution of either the pump or the dopant. One possibility is to confine the RE ions to regions where the desired signal mode has a high intensity. In the case of a conventional Gaussian-like mode, the RE ions will then be confined to the central region of the core [144,145], which is relatively straightforward, but confined doping will be more difficult for modes with complex distributions such

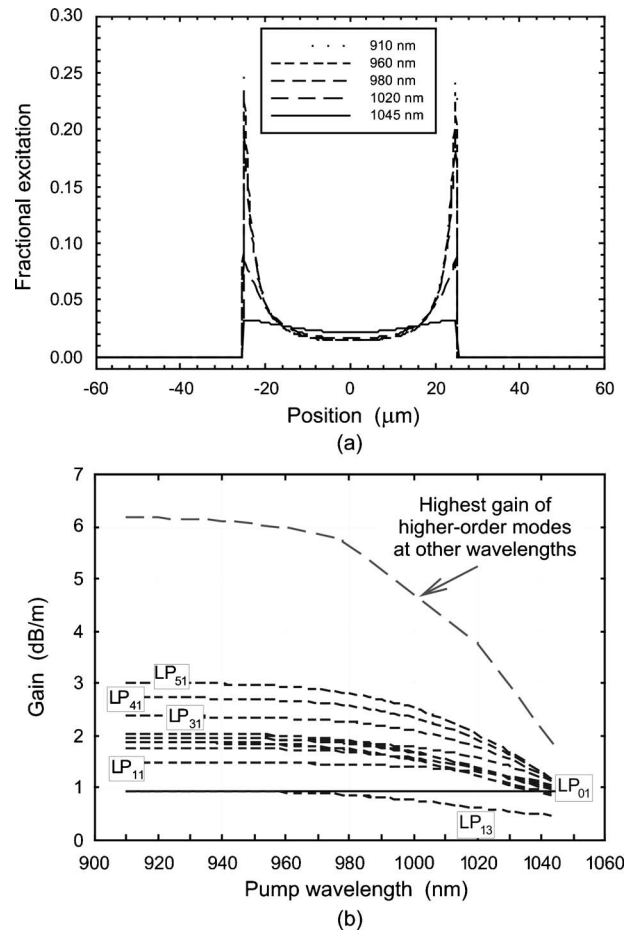


Fig. 15. (a) Fractional Yb excitation level for an ideal step-index core with a diameter of 50 μm and a NA of 0.06. All signal photons are in the fundamental mode, and all pump photons are evenly distributed across the fiber cross-section. The numbers of pump and signal photons are the same, spontaneous emission is negligible, and the pump area is adjusted for an average fractional excitation of 0.030 for the fundamental mode, corresponding to a signal gain of 0.95 dB/m. (b) Fundamental mode— LP_{01} (solid horizontal line) and HOM (dashed curves) gains at the signal wavelength, and highest gain of any HOM at any wavelength (long-dashed curve) under different pumping wavelengths with cladding area adjusted for the same fundamental mode signal gain of 0.95 dB/m [155].

as HOMs. Furthermore, modes can suffer distortion in bent fibers [157], which complicates the use of confined doping. It also reduces the pump absorption and signal gain due to the reduction in the RE-doped volume. Another possibility is to confine the pump to regions where the intensity of the desired signal mode is high [158,159]. This is most easily done with single-mode pumping and has also been demonstrated with HOMs [110]. However, single-mode pumping is a severe restriction for brightness enhancement and power scaling. Furthermore, tandem-pumping close to the emission wavelength makes the gain more uniform longitudinally as well, whereas the other approaches do not.

We have seen above that mode area scaling is critical for addressing damage and nonlinear degradation, but this is limited by imperfect mode selection, mode-coupling, and gain saturation effects in active fibers. In the high power regime, thermally induced guiding can

also limit the mode area scaling. Light propagation in fiber lasers, as defined by the refractive index distribution, has been viewed to be largely immune to thermal effects. However, at very high power levels and for laser transitions with a large quantum defect, thermally induced changes in the refractive index profile can lead to stronger mode confinement (i.e., for thermo-optic coefficient $dn/dT > 0$). This leads to lower thresholds for unwanted nonlinear loss processes (SRS and SBS) and catastrophic damage for the fundamental mode. It can also lead to a degradation in beam quality by virtue of parasitic excitation of HOMs. The maximum thermal load per unit length that can be tolerated before thermal guiding becomes an issue and is inversely proportional to the mode area [129]. Thus, in this limit, the ratio of the fiber length to the mode area will be fixed [160], which in turn implies that a larger core can no longer be used to mitigate SRS and other (third-order) nonlinearities. Under these assumptions, if SRS is the most important nonlinearity, one can show that the maximum power $P_{\text{SRS-thermal}}$ becomes [160]

$$P_{\text{SRS-thermal}} = 4\pi\lambda_L \sqrt{\frac{A_{\text{eff}}\eta_{\text{laser}}K_{\text{silica}}G_{\text{tot}}}{A_{\text{co}}2\eta_{\text{heat}}\frac{dn}{dT}g_R}}, \quad (8)$$

where η_{laser} is the laser efficiency, η_{heat} is the fraction of the pump power converted to heat, K_{silica} is the thermal conductivity of silica (i.e., for the core), G_{tot} is the total logarithmic gain in the amplifier, and g_R is the Raman gain coefficient. With the parameter values given in [160], $P_{\text{SRS-thermal}}$ becomes 36.6 kW. It is also possible to determine the optimal value of the ratio between the length and the effective area, $(L/A_{\text{eff}})_{\text{opt}}$. This becomes

$$(L/A_{\text{eff}})_{\text{opt}} = \frac{4}{\pi\lambda_L} \sqrt{\frac{A_{\text{co}}2\eta_{\text{heat}}\frac{dn}{dT}G_{\text{tot}}}{A_{\text{eff}}\eta_{\text{laser}}K_{\text{silica}}g_R}}. \quad (9)$$

With the parameters in [160], this ratio becomes 3.87 nm^{-1} . This can be compared to the ratio of the Rayleigh length to the beam area at the focus of a diffraction-limited Gaussian beam. This ratio becomes $n/\lambda_L = 1.37 \mu\text{m}^{-1}$ for a laser wavelength of 1064 nm and a refractive index n of 1.46. This is some 2800 times smaller than $(L/A_{\text{eff}})_{\text{opt}}$. We conclude, therefore, that in this ultimate limit, a waveguide is necessary for realizing the geometry that leads to the optimal balance between nonlinear (SRS) and thermal effects, as determined by fundamental material parameters. Furthermore, most dopants produce a larger thermal load than Yb, which strengthens the importance of a fiber waveguide for those other dopants.

The maximum power according to Eq. (8) is much higher than what has been reached to date, and there are of course a number of additional constraints on the fiber laser power, e.g., available pump power, thermal coating damage, and optical damage. Those constraints suggest that a long fiber with a large core should be used. However, the reduction in mode area in a bent fiber also places a practical upper limit on the core diameter, and it is clear

that these additional constraints may well limit the power much below the value of 36.6 kW suggested by Eq. (8). In particular, as discussed in [160], the core size required to avoid optical damage at 36.6 kW may be prohibitively large.

Equations (8) and (9) can be used in the pulsed regime, as well, following slight modifications to account for the more severe nonlinear effects typical for pulsed devices at a given average power. In the conventional SRS-limited case, the average power becomes

$$P_{\text{SRS-thermal}} = 4\pi\lambda_L \sqrt{\frac{A_{\text{eff}}\eta_{\text{pulse}}\eta_{\text{laser}}K_{\text{silica}}G_{\text{tot}}}{A_{\text{co}}2\eta_{\text{heat}}\frac{dn}{dT}g_R}}, \quad (10)$$

while the optimum value $(L/A_{\text{eff}})_{\text{opt}}$ is given by

$$(L/A_{\text{eff}})_{\text{opt}} = \frac{4}{\pi\lambda_L} \sqrt{\frac{A_{\text{co}}2\eta_{\text{pulse}}\eta_{\text{heat}}\frac{dn}{dT}G_{\text{tot}}}{A_{\text{eff}}\eta_{\text{laser}}K_{\text{silica}}g_R}}, \quad (11)$$

where η_{pulse} is the pulse duty cycle. We see that the optimal ratio $(L/A_{\text{eff}})_{\text{opt}}$ is proportional to the square root of the pulse duty cycle. Therefore, the difference between the optimal waveguide and a diffracting geometry becomes smaller for lower duty cycles and disappears completely for duty cycles of the order of 10^{-6} .

Single-frequency amplifiers are also limited by nonlinear scattering, in this case SBS. Using Eq. (10) with the Raman parameters replaced with the corresponding Brillouin parameters, a maximum power limit of 1.86 kW was found in [160]. The corresponding value of $(L/A_{\text{eff}})_{\text{opt}}$ becomes $178 \mu\text{m}^{-1}$, which is significantly smaller than for Raman-limited cw case operation, but still much larger than for a diffracting beam, which points to advantages of a waveguide also for high power single-frequency amplification. We note finally that in-band tandem-pumping has a role to play also in this context of ultimate power scalability, in that it helps to reduce the thermal load and thus allows for further power scaling (Eq. (8) above and [160]).

2. Reducing the Material Kerr Nonlinearity

Stepping back from the regime of very high average powers where thermal limits need to be considered, the most promising route to substantially increased nonlinear and damage thresholds for single-mode operation is to exploit hollow-core fiber technology (PBGFs [161] and Kagome fibers [162]). Such fibers offer extremely low values of optical nonlinearity per unit length—as low as one thousandth of those of conventional solid fibers by minimizing the modal overlap with the glass structure. While this is clearly of great interest for passive fiber delivery, for lasers the obvious challenge is to find a way to achieve significant gain when the modal overlap with the solid regions of the fiber is so low. One possible solution could be to move away from RE doping and to use a gaseous gain medium within the fiber core. Indeed gas-based lasers based on Raman scattering in hydrogen have now been reported (albeit pumped with high-brightness pulsed single-mode lasers) [163]. We can only hope that as

higher-brightness pump laser technology emerges, and pump coupling technology for microstructured fibers improves, that new concepts and fiber designs better able to trade off reduced nonlinearity for signal gain will emerge, and that these will allow hollow-core fiber to find application in active high power laser devices. Note that the use of hollow-core fibers also allows light to be transmitted in regions in which conventional solid fibers are strongly absorbing, e.g., in the ultraviolet (UV) and mid-IR. This also has implications for external frequency conversion schemes in these spectral regions and provides important laser delivery options across extended wavelengths.

3. Mitigation of Stimulated Inelastic Nonlinear Scattering by Fiber Design

Given a certain mode area, fiber length, and desired strength of elastic Kerr-based nonlinear interaction, it is often necessary to control the level of inelastic nonlinear scattering which is an undesirable parasitic effect in many instances. SRS suppression is an area in which photonic bandgap concepts and antiresonant guiding phenomena already look set to play a significant role. In this instance the fact that the PBGFs guide light only over a limited spectral bandwidth can be exploited to provide a large distributed inline loss at the Raman Stokes shift while presenting minimum loss at the signal wavelength. Here, solid PBGF variants can be used (allowing a solid core and thus incorporation of cladding-pumpable RE ions [164,165]). Significant increases in the SRS threshold might in principle also be possible using such an approach with optimized fiber designs and material choices, although this is much more difficult because of the small Stokes shift and the strength of SRS and may more easily be implemented using inline blazed gratings [166]. Note though, as already mentioned in Subsection 2.B, that significant work has also taken place these past years on developing acoustically engineered fibers providing a much reduced Brillouin response [47–51], and it is conceivable that such SRS suppression concepts might ultimately be simultaneously incorporated in the design of SRS suppressed fibers to provide additional functionality and opportunities to control the relative strength of different and sometimes competitive nonlinear effects. Finally, it should be mentioned that it is also possible to engineer in-band dispersion using PBGF effects which again is extremely important when managing the impact of optical nonlinearity on short optical pulses.

4. Mode Area Scaling Using Multiple Apertures—Beam Combination

Despite the exciting prospects for further power scaling discussed above, at some point the upper limit on power from a single aperture will be reached. Scaling output power in cw or pulsed mode beyond this limit can be achieved via beam combination. Well-established features of active fibers such as low cost, modular design, reliability, high efficiency, good beam quality, and high control (notably in MOPAs) are very attractive for beam combination, and there has been good progress to date. Here, our objective is limited to outlining the many different beam combination schemes in a fiber context and discussing

their scalability and suitability for different operating regimes. For technical details, we refer to a recent journal issue on the topic [37].

Beam combination can be divided into two types, incoherent and coherent beam combination, and can be applied to multi-core fibers and multiple single-core fibers. There are furthermore two versions of incoherent beam combination, the so-called spatial beam combination and spectral (or wavelength) beam combination. There are also two types of coherent beam combination distinguished by the method of phase control, i.e., active or passive. Polarization multiplexing is the simplest method for incoherent beam combination, but offers at best a factor of 2 increase in power (and brightness), so often ignored in discussions about the pros and cons of the various beam combinations schemes. The usual division into operating regimes applies as well, i.e., cw, high-energy pulses (nanoseconds), and ultrashort pulses (femtoseconds to picoseconds).

The potential benefits of beam combination are clear. First, it provides a scalable route to increase the effective core area, thereby reducing nonlinear effects within the fiber elements of the system for a given combined field intensity or power. It also reduces the corresponding in-fiber peak intensities which can be important from a damage perspective depending on the operating regime. Moreover, if the approach of separate fibers is used the overall heat load can be distributed over a number of fibers easing thermal management. However, such benefits come at a considerable cost in terms of complexity and stability of the system, and much more work will be required to try and develop simpler and more practical means to affect beam combination.

The simplest, and already quite widespread, beam combination technique is spatial beam combination (sometimes referred to as beam stacking) in the cw regime. The outputs from a number of spatially incoherent fiber sources are combined into a single beam in a fiber combiner or a free-space combiner, or are simply focused into a common focal point. Fundamentally, this is not different from the diode stacking illustrated in Fig. 12, and it offers a route to virtually any desired power level albeit at the expense of poorer beam quality and a small reduction in brightness. This approach is used for industrial lasers up to 50 kW of output power [124], and even after combination, the beam quality can still be sufficiently good for demanding industrial and defense applications (e.g., short-range directed energy [167]).

Spatial beam combination can also be used for nanoscale-scale high-energy pulses. In this case, the only additional complication is pulse timing. This suggests that a multi-path MOPA configuration consisting of many parallel high-energy amplifiers seeded by a common pulsed laser should be used. A pulse duration of 1 ns corresponds to 20 cm of fiber propagation, so the fiber lengths need to be adjusted on this scale to synchronize pulses from all channels. For ultrashort pulses (say 1 ps), the length matching becomes more critical with a tolerance of the order of 0.2 mm. At such tolerances, thermally induced variations of the refractive index need to be considered. For example, with a fiber path of 10 m, a temperature change of 2 K is enough to change the optical

path length by 0.2 mm. Differences in temperature between different arms on this scale are easy to envisage, so precise control of the temperature or, more directly, of the optical path length is likely to be required for incoherent combination of picosecond-scale pulses amplified in separate fiber arms.

The path-length difference due to different fiber lengths as well as to temperature differences may be easier to manage with a multi-core fiber, allowing the different channels to be amplified in different cores. The fiber geometry and heat-sinking arrangement is important for minimizing temperature differences between cores. A ribbon fiber with a linear array of cores should be attractive for this purpose, but the thermal limit on average power will obviously be lower than for an arrangement with separate fibers.

Spectral beam combination is a more sophisticated incoherent technique, in which several beams of (typically) similar beam quality but at different wavelengths are wavelength-multiplexed into a single combined beam with beam quality similar to that for an individual (constituent) beam. Thus, the spatial brightness can be increased significantly via this approach. The wavelengths of the different emitters can either be determined by conventional means (e.g., MOPAs seeded at the desired wavelengths) or the beam-combination arrangement can be located within a common external feedback cavity. In the latter case, the cavity automatically selects the correct wavelength for each emitter.

The elements for combining (i.e., wavelength multiplexing) are crucial for spectral beam combination. Diffraction-gratings, VBGs, interference filters, and polarization combining followed by wavelength-dependent polarization rotation are popular multiplexing elements. With a diffraction-grating, the beam combination can be performed in a single step with the incident angles of the different beams arranged such that all the diffracted beams emerge in a single direction. In addition, the beams to be combined need to be incident on the same spot on the grating and lie in a plane. This is a good match for ribbon fibers, although the number of cores, and therefore the scalability, will always be quite limited in a single multi-core fiber configuration. The other combination approaches involve cascaded combination with beams arriving from different directions, so they seem better suited for combination of conventional single-core fibers.

The upper limit on power attainable via this approach depends on power handling and cascadability of the combining elements, obtainable spectral channel density, power and linewidth achievable from the individual fiber emitters, and the bandwidth over which they can operate. Looking forward, it seems safe to assume that in the cw regime, linewidths of a small fraction of a nanometer should be achievable at the multi-kilowatt level and possibly beyond from near-diffraction-limited Yb-doped fiber sources. Therefore, it appears that the combining elements rather than the fiber sources will determine how many fiber sources that can be combined and the ultimate limit on power. This is particularly so when one considers that high power radiation can be generated with various linewidths all the way from 1 to 2 μm , using a combina-

tion of Yb-, Er-, and Tm-doped fiber sources as well as Raman sources, and perhaps using a combination of coarse and fine wavelength multiplexing. Indeed, the wavelength agility of fiber sources is a prime attraction for spectral beam combination.

Still, the power levels used to date appear to be far below what the best multiplexing arrangements can handle. For example, a normal surface relief grating should allow over 100 Yb-doped fiber sources to be combined to a power of 100 kW [168], and probably well beyond, limited by financial constraints rather than technical ones for the foreseeable future.

In the pulsed regime, spectral beam combination of individually wavelength-locked lasers requires careful control and synchronization of pulses from the constituent fiber sources. This is a practical issue, but will become increasingly challenging to address as the number of sources to be combined increases and pulse durations decrease. To date, only four channels have been wavelength-multiplexed in the nanosecond regime [169]. It may be better to use a beam-combined multi-wavelength cw seed laser and a modulator to generate pulses followed by wavelength-demultiplexed amplification and subsequent spectral recombination. See reference [168] for a cw example of a similar configuration (albeit without intermediate multiplexing and demultiplexing).

As for beam stacking, combining of ultrashort pulses will be more challenging due to the required path-length matching. Furthermore, the bandwidth of ultrashort pulses needs to be considered as well, given the limited channel bandwidth as well as spatial and/or temporal dispersion effects. Therefore spectral beam combination looks less than ideal for ultrashort pulses.

Coherent beam combination is quite different in many respects. In passive phasing, a number of gain-fiber arms share a common cavity, but in contrast to the intracavity spectral beam combination, the combining element is not wavelength-selective, and the gain fibers all operate at the same wavelength. Furthermore, instead of the gain arms operating independently as they do for spectral beam combination, the combining arrangement actually couples the gain arms to each other. The passively phased laser array can then be understood to be operating on a single super-mode of the multiple fibers. It is possible to design the cavity so that it selects a desired super-mode by ensuring that this has the lowest loss of all possible super-modes. This super-mode is then coupled to a single, normally diffraction-limited, mode at the output of the cavity. In the low power regime, a single-mode fiber can be used for this purpose, and an arrayed cavity can be formed by cascading conventional single-mode fused-fiber couplers [170]. At higher powers, non-waveguiding approaches are needed, e.g., employing a MM fiber structure [171], an external reflector setup in a Talbot or self-Fourier configuration [172], or a Damman grating [173]. Some of these arrangements, notably the Talbot cavity, are also attractive for phasing of multiple cores in a single fiber [174].

In order to avoid excess loss for the desired (lowest-loss) super-mode, the round-trip phases in all gain arms must be the same, bar for multiples of 2π . Herein lies the challenge with passive phasing, as this phase is not con-

trolled. Nevertheless, due to a degree of spectral freedom of the phased array, the phase condition can largely be fulfilled up to array sizes of approximately ten [175–177], as the array finds a wavelength that minimizes the loss of the super-mode. Furthermore, it is possible to design cavities with relaxed sensitivity to phase errors [178], although the power scalability of this approach, and indeed the ability to achieve effective passive phasing, remains to be determined.

An array of the order of ten gain fibers, or cores, does represent significant scaling but is still quite limited. We note however that in contrast to other combination schemes, important aspects of the physics of passive phasing are not well understood, and there may be opportunities for utilizing optical nonlinearities [179,180], for example, to phase-lock the arms and scale to larger arrays. However it should be appreciated that there are several nonlinear effects in a fiber with different temporal characteristics, i.e., the Kerr nonlinearity, electrostriction, thermal effects, and gain-inversion effects according to the Kramers–Kronig (KK) relation. These nonlinearities have to be better understood if they are to be exploited for phase-locking. On the other hand, in a multi-core fiber, conventional linear distributed coupling between cores can also be used for phase-locking [179]. To date passively phased fibers lasers with as many as 16 cores have been demonstrated using this approach [174].

It is interesting also to consider to what extent a larger laser bandwidth (as determined by the gain medium and the cavity) allows for a larger array due to the higher probability of finding a wavelength with a small phase error. In fact, this relation is not very strong, allowing—arguably—only for logarithmic growth in the array size. A better approach may be to use a small array of perhaps five arms, restricted to a narrow wavelength range, and then to spectrally beam-combine a number of such arrays for further power scaling.

As it comes to pulsing, although a passively phased array could be mode-locked in theory this would appear very difficult in practice. This would preclude ultrashort pulse operation. Also nanosecond-scale operation would appear to be problematic due to the nonlinear phase shifts that occur at high peak powers. Intriguingly, though, promising results have been reported, albeit with only two channels [181]. A simple, passive, and scalable solution in this area would be very interesting since beam combining in the pulsed regime is generally quite challenging and complex.

Active phasing is the engineering approach to coherent beam combination. Here, the light from a single seed source is split and amplified in several arms, and then coherently recombined. The combination can take place in some element such as a Damann grating [182] or a self-imaging waveguide [183]. Alternatively, the beams can be stacked side by side in a phased array, which then forms a diffraction-limited beam (subject to fill-factor limitations) and which can also be controlled (steered) to a degree. In this case, there is no discrete combining element. Active phasing does involve difficult challenges, but the phase control problem appears to be solved (see, e.g., [184]). The stability of the mounted array does remain an issue, but is being addressed and is not a long-term concern. Also

SBS is being addressed: active phasing becomes easier with highly coherent sources, as this allows for longer path-length differences between arms of multiples of 2π . However, high temporal coherence can lead to SBS, but there has been very good progress in SBS suppression and power scaling of narrow-line sources in recent years, as discussed in Subsection 2.B.

Active phasing is very attractive from a scalability point of view. Although stringent (e.g., $\lambda/20$) phase control is required, this tolerance is independent of the number of elements.

In the pulsed regime, the high energies targeted for nanosecond pulsed sources may well lead to difficult-to-control variations in nonlinear phase shifts between different arms, although this will be less of an issue for longer pulses of, say, 100 ns duration. Even then, though, the change in KK-related change in the refractive index is a concern, and it clearly requires very precise control of the system to ensure that the nonlinearities in different arms are balanced. Coherent combination of ultrashort pulsed sources, although again requiring precise path-length matching (i.e., the number of 2π phase differences tolerated is relatively small), could conceivably be simpler in that the pulse energy is smaller and CPA can be used to keep the peak power down. Once again, a single multi-core fiber is attractive for ultrashort pulses, in that it helps to keep the path-length differences small [185]. As an illustration of the advantages that this can bring, consider the 16-core fiber laser, passively phased in a Talbot cavity reported in [179]. This had an effective area exceeding $5000 \mu\text{m}^2$ for operation on the fundamental super-mode at $1.06 \mu\text{m}$. Applying these approaches with ultra-large mode area fiber designs, e.g., leakage channel fibers [186], to allow operation at effective areas well beyond $10,000 \mu\text{m}^2$ will be increasingly important moving forward—most particularly for pulsed laser systems where managing the high peak powers is the primary issue and thermal effects are secondary.

To summarize, although it seems unlikely that all of these alternatives will be pursued successfully in the future, it is clear that some of them will be, providing different advantages for different applications, considerable diversity, and a greatly expanded range of options for the laser engineer to choose from. Although the requirements on the gain fiber differ for different combination architectures, to reduce complexity it still looks attractive to develop standardized fiber building blocks that can be used for several architectures.

5. Nonlinear Mitigation through Pulse Shape Control

Kerr effects are ultrafast and therefore manifest themselves instantaneously across a pulse as it is amplified. Consequently, if one can accurately shape an optical pulse, it becomes possible in theory to control the evolution and consequent impact of SPM. In this regard various simple pulse forms are of interest—for example, rectangular pulses simply generate a uniform phase shift across their envelope under the influence of SPM, and the only frequency-chirp (which compromises pulse quality) is generated at the leading and trailing edges. If these edges are sufficiently abrupt, then the relative impact of SPM can be modest, particularly if the chirped frequency com-

ponents can be filtered away at the system output. Parabolic shaped pulses generate linear chirps under the influence of SPM that can subsequently be removed using dispersive elements such as grating and prism pairs. In principle, with adequate temporal control SPM can be mitigated reasonably well in many instances of practical interest [187], leaving SRS as the primary nonlinearity to address. However, even here, pulse shaping can be gainfully used. For example, square optical pulses experience uniform SRS gain across their envelope which either can be exploited to ensure that maximum pulse energy is extracted from an amplifier before the onset of SRS [73], or indeed can be used as an efficient pulsed wavelength conversion mechanism [188].

A number of pulse shaping technologies are now readily available, and in the coming decade we envisage increasing use of these in advanced fiber laser systems in order to mitigate, or indeed exploit, fiber nonlinearity. In terms of fixed-response (and potentially low-cost) pulse shapers we highlight superstructured fiber Bragg grating [189] and long period grating [190] technology which have been used for many years in telecommunications applications to perform complex pulse shaping functions (including the generation of both square and parabolic pulses). In terms of adaptive filters we point to products such as the Wave-shaper from Finisar Inc. based on liquid crystal technology which provides for signal phase and amplitude control with very good (~ 5 GHz) spectral resolution [191]. AO and conventional spatial light modulator based devices as used extensively with Ti:sapphire-based femtosecond laser systems are also becoming commercially available at relevant fiber laser wavelengths.

We believe that the combination of pulse shaping along with nonlinearity/dispersion engineered fibers will offer many interesting device and system applications in the forthcoming decade and will provide a rich opportunity for significant further innovation. Obviously, once developed for single-core operation these concepts should readily be extendable to the multi-aperture regime to allow further power scaling there also.

6. Adaptive Fiber Laser Systems

With the emergence of adaptive pulse shaping technology capable of operating over extended time scales from the femtosecond to effectively the cw regime and the relative flexibility and transparency of MOPAs, the possibility of creating adaptive, yet practical and affordable, laser systems capable of optimizing their output parameters to suit a given application comes to mind. Indeed, considerable work on developing sources with pulse shapes optimized for particular applications, such as the color-marking of metals, has already been undertaken. We believe that this is just the tip of the iceberg and that this will be an increasing theme of fiber laser research in the coming decade. One can envisage intelligent self-learning lasers, for example, receiving information back on cutting quality, or speed, and automatically adapting their output characteristics over relatively wide operating ranges using suitable learning algorithms to optimize application performance. One can even envisage incorporating some form of spatial mode optimization into the laser design—for example, some applications require ring type or flat-

top beams, which may be obtained by suitable mode-engineering or post-processing of the fiber facet. The use of a wavelength selective mode converter at the fiber output with wavelength tuning of the input seed laser might even allow for a degree of dynamic control. The whole area of wavelength agility at the seed laser coupled with wavelength selective elements within a MOPA system opens up a host of new device opportunities.

D. Other Wavelengths

The methods and concepts we have discussed so far are particularly relevant for lasers that operate close to thermal, nonlinear, and optical damage limits. However, another priority is to extend the wavelength coverage of high power fiber sources. The challenges here can be similar to those for Yb power scaling, but they can also be quite different; but regardless, it is apparent that improved operation on other laser transitions is sure to follow in due course. Indeed, recent advances in power scaling of Tm-doped silica fibers to kilowatt power levels in the ~ 2 μm wavelength regime bear strong testimony to this, and further advances are to be anticipated here. Coverage of much of the near infrared band from ~ 0.9 to ~ 2.1 μm can be achieved using RE ion transitions in silica and non-silica fibers supplemented where necessary by Raman shifting. The advent of silica fibers doped with bismuth [192] (a so-called poor metal rather than a RE) has opened up the difficult-to-access wavelength regime from ~ 1140 to ~ 1500 nm, complementing the spectral range available from RE-doped fibers. Power levels are quite modest at the moment [193], but the prospects for scaling to much higher power using in-band pumping schemes based on the use of one or more Yb fiber pump lasers look promising. It is also worth mentioning the prospects of other dopants, e.g., lead and chromium. A range of dopants have been investigated extensively in the past, with limited success, but advances in fabrication techniques such as nano-crystals [194] can be used to modify and control the local environment of the active centers. In this way, all transitions demonstrated in crystals can conceivably be realized in fibers as well.

Operation on laser transitions in the visible and mid-infrared bands is much more challenging, and as a consequence both output power and spectral coverage are rather limited. At wavelengths beyond ~ 2.2 μm , the attenuation coefficient for silica increases dramatically, and hence other glass hosts (e.g., fluorides [195], tellurites [196], and chalcogenides [197]) with superior infrared transmission are required. These glasses also benefit from lower phonon energies than silica, but fabrication of low-loss fibers (active and passive) is an obvious challenge as is the fabrication of associated fiberized components. Much of the work on mid-IR fiber lasers has focused on Ho-doped ZBLAN (ZrF_4 - BaF_2 - LaF_3 - AlF_3 - NaF) [198] and Er-doped ZBLAN [199] lasers operating in 2.70–2.83 and 2.85–2.95 μm bands, respectively. Development of these lasers has been driven mainly by the prospect of a range of applications in the biomedical area exploiting the strong absorption band in water at ~ 3 μm . To date, the maximum output power reported for a cladding-pumped Er:ZBLAN fiber laser is 24 W for 166 W of diode pump power at ~ 975 nm [200]. The combination of low effi-

ciency, high thermal loading density, and the relatively poor thermo-mechanical and optical damage properties of the mid-IR glass hosts compared to silica will make further power scaling very challenging.

An alternative strategy for extending the range of operating wavelengths to the mid-IR is offered by the hybrid fiber-bulk-laser architecture. In this approach, a high power fiber laser operating in the near-IR wavelength regime is used as a high-brightness pump source for a bulk crystal laser. There are a number of fiber-bulk-laser combinations that can yield output in the mid-IR regime. One notable example is Tm- or Er-fiber-laser-pumped Cr:ZnSe [201], which offers access to a broad range of operating wavelengths in the $\sim 2\text{--}3\ \mu\text{m}$ band [202]. Also, a relatively new material, Fe:ZnSe, offers laser emission in the $3.95\text{--}5.05\ \mu\text{m}$ band [203]. As with many bulk laser configurations thermal loading and its deleterious effects represent a major challenge to power scaling, particularly in laser configurations such as these where quantum defect heating is high.

In many respects the most straightforward way to extend the range of operating wavelengths to the visible and mid-IR bands is via external nonlinear devices (i.e., second-harmonic generators, optical parametric oscillators and amplifiers, and both difference frequency and sum generators). However, the pump requirements for efficient nonlinear conversion such as high power, narrow linewidth, and single polarization are not always easy to satisfy simultaneously in a fiber geometry at high average power and may result in significant added complexity to the fiber system. Tailoring fiber designs and systems to meet these needs is very much an ongoing research activity, motivated by the prospect of access to virtually any wavelength in the UV-visible [204,205] and near mid-IR [206] wavelength regimes at high average power to complement the spectral coverage offered by fiber lasers themselves in the near IR. Already, using this approach pulsed Yb fiber MOPAs have been frequency-doubled to generate over 80 W of green at 530 nm [207]. Increasing fiber laser power levels, spectral densities, and wavelength coverage for different pulse duration regimes is sure to figure as a major area of research activity for the foreseeable future, yielding—via nonlinear frequency conversion—light at wavelengths spanning the soft x-ray to terahertz regimes.

6. CONCLUSIONS

In conclusion, we have reviewed the current state of the art in fiber laser technology in relation to both parametric performance and practical considerations such as thermal and damage management. Our review has highlighted that, in both continuous-wave (cw) and indeed many forms of pulsed operation, the results for ytterbium fiber laser are close (within perhaps a factor of 2–3), of significant fundamental limits for single-mode operation using the existing technology. However, we note that plenty of scope remains for translating knowledge and experience gained here to high power lasers based on the less developed Er-, Tm-, Ho-, and Nd-based transitions—indeed, given the recent progress, it will be interesting to see whether the ultrahigh efficiencies obtainable in ytterbium

means that this RE system will win out in terms of achieving the highest possible power levels or whether the larger mode areas achievable in thulium will prove decisive despite the lower power efficiency.

Looking forward to the next decade we have speculated as to how developments in the existing underpinning pump, fiber fabrication, and component technologies are likely to impact the development of fiber laser technology and have given some personal thoughts as to how new and emerging forms of fiber and new system architectures and concepts may extend the performance range and applicability of the fiber approach. Extending the mode size while obtaining robust performance is arguably the most critical issue in power scaling both pulsed and cw lasers, and radical innovation will be required here if the rate of power growth from single-aperture lasers enjoyed this past decade is to be maintained long into the next. Clearly, single-modedness is not essential for all applications of high power lasers, and therefore more systematic study and understanding of the power scaling limits versus trade-offs in terms of thermal/damage management, mode quality, and stability are also required for MM fibers, not least in developing a better understanding of the impact of mode competition and relative modal excitation levels on pointing stability and damage thresholds. In pushing to the highest possible power levels, it is to be appreciated that ensuring long-term reliable operation is likely to be highly challenging, and it may well be that the practical limit for reliable commercial systems will always be a significant factor down on the record levels set in the laboratory. Hopefully, this down-rating will be minimized as greater understanding and appreciation of possible failure modes under high power operation of fibers (and associated components) are developed. Clearly, improvement in the power handling of isolators, pump combiners, gratings, optical coatings, and indeed the fibers themselves will be essential to the continued commercialization of the technology as power levels continue to increase.

In terms of pulsed laser performance improvements in large mode area fibers (for reduced device lengths, nonlinearity, and susceptibility to damage) are likely to lead to further increases in the pulse energies and peak powers that can be derived from fiber systems. 100 mJ Q-switched and multi-millijoule femtosecond systems are within sight by exploiting emerging techniques for nonlinearity and dispersion control. The use of adaptive pulse shaping techniques in fiber MOPA systems are also coming to the fore—promising designer pulse shapes at high average powers for pulses with durations spanning the millisecond to femtosecond regimes. The possibility of using spatial mode shaping, of either diffraction-limited beams or indeed heavily multimode (MM) beams, provides further exciting possibilities. Initial results in this direction are beginning to emerge using both bulk- and fiber-based mode shaping approaches. Combining both temporal and spatial beam shaping in fiber MOPAs provides perhaps one of the most intriguing and exciting opportunities for future research, leading to the prospect of MOPA-based laser sources providing adaptive control of spatio-temporal laser fields at high peak and average powers. Combining such advanced lasers with suitable

feedback and adaptive algorithms should lead to lasers that will self-optimize their outputs to suit particular end applications—greatly enhancing process efficiency and control. Clearly many challenges lie ahead in attempting to realize such concepts in practice; however opportunities to make significant in-roads in this direction clearly exist and will certainly be exploited in the coming decade.

Once the single-aperture power limits are reached then the only real option for further power scaling will be to look at beam combination. As we have reviewed, numerous technical approaches exist including coherent or incoherent, active or passive, and multi-core fibers or multiple single-core fibers. One should expect substantial activity in these areas in the coming decade, and significant progress should be anticipated in both cw and pulsed regimes.

With options for improved wavelength coverage afforded by new glass types and advances in external frequency conversion from the soft X-ray to terahertz regimes, the future opportunities for fiber laser research and further commercialization appear very bright indeed.

ACKNOWLEDGMENTS

The authors are deeply indebted to their many colleagues, collaborators, and sponsors for many useful discussions and interactions over the years which have undoubtedly helped inform and shape this article. To acknowledge each would be impossible in the space available; however we would like to thank in particular Professor David Payne, Professor David Hanna, Professor Michalis Zervas, and Professor David Shepherd, and Dr. Jayanta Sahu, Dr. Yoonchan Jeong, Dr. Christophe Codemard, Dr. Jonathan Price, Dr. Andrew Malinowski, and Dr. Shaiful Alam for particularly helpful discussions during the time of preparation of this manuscript. In addition, we gratefully acknowledge the United Kingdom Engineering and Physical Sciences Research Council (EPSRC) for sustained funding over many years for our work in the area of fiber laser and amplifier technology.

REFERENCES

- H. M. Pask, R. J. Carman, D. C. Hanna, A. C. Tropper, C. J. MacKechnie, P. R. Barber, and J. M. Dawes, "Ytterbium-doped silica fiber lasers—versatile sources for the 1–1.2 μm region," *IEEE J. Sel. Top. Quantum Electron.* **1**, 2–13 (1995).
- R. Paschotta, J. Nilsson, A. C. Tropper, and D. C. Hanna, "Ytterbium-doped fiber amplifiers," *IEEE J. Quantum Electron.* **33**, 1049–1056 (1997).
- Y. Jeong, J. K. Sahu, D. N. Payne, and J. Nilsson, "Ytterbium-doped large-core fiber laser with 1.36 kW continuous-wave output power," *Opt. Express* **12**, 6088–6092 (2004).
- J. Nilsson, S. Ramachandran, T. M. Shay, and A. Shirakawa, "High-power fiber lasers," *IEEE J. Sel. Top. Quantum Electron.* **15**, 1–2 (2009).
- Y. Jeong, A. J. Boyland, J. K. Sahu, S. Chung, J. Nilsson, and D. N. Payne, "Multi-kilowatt single-mode ytterbium-doped large-core fiber laser," *J. Opt. Soc. Korea* **13**, 416–422 (2009).
- R. W. Berdine and R. A. Motes, *Introduction to High Power Fiber Lasers*, 1st ed. (Directed Energy Professional Society, 2009).
- E. Snitzer, "Proposed fiber cavities for optical lasers," *J. Appl. Phys.* **32**, 36–39 (1961).
- E. Snitzer, "Optical maser action of Nd^{3+} in a barium crown glass," *Phys. Rev. Lett.* **7**, 444–446 (1961).
- C. J. Koester and E. Snitzer, "Amplification in a fiber laser," *Appl. Opt.* **3**, 1182–1186 (1964).
- J. Stone and C. A. Burrus, "Neodymium-doped silica lasers in end-pumped fiber geometry," *Appl. Phys. Lett.* **23**, 388–389 (1973).
- S. B. Poole, D. N. Payne, and M. E. Fermann, "Fabrication of low loss optical fibres containing rare-earth ions," *Electron. Lett.* **21**, 737–738 (1985).
- R. J. Mears, L. Reekie, S. B. Poole, and D. N. Payne, "Neodymium-doped silica single-mode fibre laser," *Electron. Lett.* **21**, 738–740 (1985).
- R. J. Mears, L. Reekie, I. M. Jauncey, and D. N. Payne, "Low-noise erbium-doped fibre amplifier operating at 1.54 μm ," *Electron. Lett.* **23**, 1026–1028 (1987).
- E. Stiles, "New developments in IPG fiber laser technology," in *Proceedings of the 5th International Workshop on Fiber Lasers* (2009).
- D. C. Hanna, R. M. Percival, I. R. Perry, R. G. Smart, P. J. Suni, and A. C. Tropper, "An Yb-doped monomode fiber laser: broadly tunable operation from 1.010 μm to 1.162 μm and three-level operation at 974 nm," *J. Mod. Opt.* **37**, 517–525 (1990).
- R. Selvas, K. H. Ylä-Jarkko, J. K. Sahu, L.-B. Fu, J. N. Jang, J. Nilsson, S. U. Alam, P. W. Turner, J. Moore, and A. B. Grudinin, "High power, low noise, Yb-doped, cladding-pumped, three-level fiber sources at 980 nm," *Opt. Lett.* **28**, 1093–1095 (2003).
- J. Boulet, Y. Zaouter, R. Desmarchelier, M. Cazaux, F. Salin, J. Saby, R. Bello-Doua, and E. Cormier, "High power ytterbium-doped rod-type three-level photonic crystal fiber laser," *Opt. Express* **16**, 17891–17902 (2008).
- F. Roeser, C. Jauregui, J. Limpert, and A. Tünnermann, "94 W 980 nm high brightness Yb-doped fiber laser," *Opt. Express* **16**, 17310–17318 (2008).
- A. Shirakawa, C. B. T. Olausson, M. Chen, K. I. Ueda, J. K. Lyngsø, and J. Broeng, "Power-scalable photonic bandgap fiber sources with 167 W, 1178 nm and 14.5 W, 589 nm radiations," in *Advanced Solid State Photonics*, 2010 OSA Technical Digest Series (Optical Society of America, 2010), postdeadline paper APDP6.
- J. K. Sahu, C. C. Renaud, K. Furusawa, R. Selvas, J. A. Alvarez-Chavez, D. J. Richardson, and J. Nilsson, "Jacketed air clad cladding pumped ytterbium doped fibre laser with wide tuning range," *Electron. Lett.* **37**, 1116–1117 (2001).
- J. D. Minelly, R. I. Laming, J. E. Townsend, W. L. Barnes, E. R. Taylor, K. P. Jedrzejewski, and D. N. Payne, "High-gain fibre power amplifier tandem-pumped by a 3 W multi-stripe diode," in *Optical Fiber Communications Conference*, 1992 OSA Technical Digest Series (Optical Society of America, 1992), pp. 32–33.
- M. L. Osowski, W. Hu, R. M. Lammert, S. W. Oh, P. T. Rudy, T. Stakelon, and J. E. Ungar, "Advances in high-brightness semiconductor lasers," *Proc. SPIE* **6876**, 68761E (2008).
- R. D. Maurer, "Optical waveguide light source," U.S. patent 3,808,549 (30 April 1974).
- J. D. Kafka, "Laser diode pumped fiber laser with pump cavity," U.S. patent 4,829,529 (5 September 1989).
- E. Snitzer, H. Po, F. Hakimi, R. Tumminelli, and B. C. McCollum, "Double-clad, offset core Nd fiber laser," in *Optical Fiber Sensors*, 1998 OSA Technical Digest Series (Optical Society of America, 1998), paper PD5.
- J. Nilsson, "Recent progress and limiting factors in high power fiber laser technology," in *Proceedings of the Conference on Lasers and Electro-Optics*, 2010 OSA Technical Digest Series (Optical Society of America, 2010), tutorial paper CTuC1.
- J. D. Minelly, W. L. Barnes, R. I. Laming, P. R. Morkel, J. E. Townsend, S. G. Grubb, and D. N. Payne, "Diode-array pumping of $\text{Er}^{3+}/\text{Yb}^{3+}$ co-doped fibre lasers and amplifiers," *IEEE Photon. Technol. Lett.* **5**, 301–303 (1993).

28. G. G. Vienne, J. E. Caplen, L. Dong, J. D. Minelly, J. Nilsson, and D. N. Payne, "Fabrication and characterization of $\text{Yb}^{3+}:\text{Er}^{3+}$ phosphosilicate fibers for lasers," *J. Lightwave Technol.* **16**, 1990–2001 (1998).
29. M. Laroche, S. Girard, J. K. Sahu, W. A. Clarkson, and J. Nilsson, "Accurate efficiency calculation of energy transfer processes in phosphosilicate $\text{Er}^{3+}-\text{Yb}^{3+}$ codoped fibers," *J. Opt. Soc. Am. B* **23**, 195–202 (2006).
30. H. Zellmer, A. Tünnermann, H. Welling, and V. Reichel, "Double-clad fiber laser with 30 W output power," in *Optical Amplifiers and Their Applications*, Vol. 16 of OSA Trends in Optics and Photonics Series (Optical Society of America, 1997), p. 137.
31. K.-I. Ueda, H. Sekiguchi, and H. Kan, "1 kW CW output from fiber-embedded disk lasers," in *Proceedings of the Conference on Lasers and Electro-Optics*, 2002 OSA Technical Digest Series (Optical Society of America, 2002), postdeadline paper CPDC4.
32. V. Dominic, S. MacCormack, R. Waarts, S. Sanders, S. Bicknese, R. Dohle, E. Wolak, P. S. Yeh, and E. Zucker, "110 W fibre laser," *Electron. Lett.* **35**, 1158–1160 (1999).
33. Y. Jeong, J. K. Sahu, D. N. Payne, and J. Nilsson, "Ytterbium-doped large-core fibre laser with 1 kW of continuous-wave output power," *Electron. Lett.* **40**, 470–472 (2004).
34. A. B. Grudinin, P. W. Turner, M. Ibsen, M. K. Durkin, J. Nilsson, D. N. Payne, and M. N. Zervas, "Multi-fibre arrangements for high-power fibre lasers and amplifiers," U.S. patent 6,826,335 (30 November 2004).
35. R. Horley, S. Norman, and M. N. Zervas, "Progress and development in fibre laser technology," *Proc. SPIE* **6738**, K7380–K7386 (2007).
36. V. Gapontsev, D. Gapontsev, N. Platonov, O. Shkurikhin, V. Fomin, A. Mashkin, M. Abramov, and S. Ferin, "2 kW CW ytterbium fiber laser with record diffraction-limited brightness," in *Proceedings of the European Conference on Lasers and Electro Optics* (2005), paper CJ-1-1-THU.
37. J. R. Leger, J. Nilsson, J. P. Huignard, A. P. Napartovich, T. M. Shay, and A. Shirakawa, "Laser beam combining and fiber laser systems," *IEEE J. Sel. Top. Quantum Electron.* **15**, 237–239 (2009).
38. R. G. Smith, "Optical power handling capacity of low loss optical fibers as determined by stimulated Raman and Brillouin scattering," *Appl. Opt.* **11**, 2489–2494 (1972).
39. R. W. Boyd, *Nonlinear Optics* (Academic, 1992), Chap. 8.
40. G. P. Agrawal, *Nonlinear Fiber Optics*, 4th ed. (Academic, 2006).
41. Y. Jeong, J. Nilsson, J. K. Sahu, D. N. Payne, R. Horley, L. M. B. Hickey, and P. W. Turner, "Power scaling of single-frequency ytterbium-doped fiber master oscillator power amplifier sources up to 500 W," *IEEE J. Sel. Top. Quantum Electron.* **13**, 546–551 (2007).
42. A. Liem, J. Limpert, H. Zellmer, and A. Tünnermann, "100-W single-frequency master-oscillator fiber power amplifier," *Opt. Lett.* **28**, 1537–1539 (2003).
43. T. Horiguchi, T. Kurashima, and M. Tateda, "Tensile strain dependence of Brillouin frequency shift in silica optical fibers," *IEEE Photon. Technol. Lett.* **1**, 107–108 (1989).
44. E. Lichtman, R. G. Waarts, and A. A. Friesem, "Stimulated Brillouin scattering excited by a modulated pump wave in single-mode fibers," *J. Lightwave Technol.* **7**, 171–174 (1989).
45. Y. Jeong, J. Nilsson, J. K. Sahu, D. B. S. Soh, C. Alegria, P. Dupriez, C. A. Codemard, D. N. Payne, R. Horley, L. M. B. Hickey, L. Wanzycy, C. E. Chryssou, J. A. Alvarez-Chavez, and P. W. Turner, "Single-frequency, single-mode, plane-polarized ytterbium-doped fiber master oscillator power amplifier source with 264 W of output power," *Opt. Lett.* **30**, 459–461 (2005).
46. R. Horley, S.-U. Alam, L. Cooper, J. Shaw, I. Mitchell, C. Sheehan, M. N. Zervas, K. Dzurko, J. K. Sahu, J. Nilsson and D. N. Payne, Y. Jeong, J.-N. Maran, C. A. Codemard, and S. Yoo, "Exploration of performance limits of fiber laser technology for directed energy applications," in *Solid State and Diode Laser Technology Review* (2008).
47. Y. Koyamada, S. Sato, S. Nakamura, H. Sotobayashi, and W. Chujo, "Simulating and designing Brillouin gain spectrum in single mode fibers," *J. Lightwave Technol.* **22**, 631–639 (2004).
48. P. D. Dragic, C. H. Liu, G. C. Papen, and A. Galvanauskas, "Optical fiber with an acoustic guiding layer for stimulated Brillouin scattering suppression," in *Proceedings of the Conference on Lasers and Electro-Optics*, 2005 OSA Technical Digest Series (Optical Society of America, 2005), paper CThZ3.
49. M. Li, X. Chen, J. Wang, S. Gray, A. Liu, J. A. Demeritt, A. B. Ruffin, A. M. Crowley, D. T. Walton, and L. A. Zenteno, "Al/Ge co-doped large mode area fiber with high SBS threshold," *Opt. Express* **15**, 8290–8299 (2007).
50. M. D. Mermelstein, M. J. Andrejco, J. Fini, A. Yablon, C. Headley, D. J. DiGiovanni, and A. H. McCurdy, "11.2 dB SBS gain suppression in a large mode area Yb-doped optical fiber," *Proc. SPIE* **6873**, U63–U69 (2008).
51. S. Yoo, C. A. Codemard, Y. Jeong, J. K. Sahu, and J. Nilsson, "Analysis and optimization of acoustic speed profiles with large transverse variations for mitigation of stimulated Brillouin scattering in optical fibers," *Appl. Opt.* **49**, 1388–1399 (2010).
52. R. J. Mears, L. Reekie, S. B. Poole, and D. N. Payne, "Low-threshold tunable-CW and Q-switched fiber laser operating at 1.55 μm ," *Electron. Lett.* **22**, 159–160 (1986).
53. D. Taverner, D. J. Richardson, L. Dong, J. E. Caplen, K. Williams, and R. V. Pentyl, "158- μJ pulses from a single-transverse-mode, large-mode-area erbium-doped fiber amplifier," *Opt. Lett.* **22**, 378–380 (1997).
54. I. N. Duling III, *Compact Sources of Ultrashort Pulses*, Vol. 18 of Cambridge Studies in Modern Optics (Cambridge University Press, 2005).
55. F. W. Wise, A. Chong, and W. H. Renninger, "High-energy femtosecond fiber lasers based on pulse propagation at normal dispersion," *Laser Photonics Rev.* **2**, 58–73 (2008).
56. T. Pfeiffer and G. Veith, "40 GHz pulse generation using a widely tunable all-polarization preserving erbium fiber ring laser," *Electron. Lett.* **29**, 1849–1850 (1993).
57. S. V. Chernikov, E. M. Dianov, D. J. Richardson, and D. N. Payne, "Soliton pulse-compression in dispersion-decreasing fiber," *Opt. Lett.* **18**, 476–478 (1993).
58. A. B. Grudinin, D. J. Richardson, and D. N. Payne, "Passive harmonic mode locking of a fiber soliton ring laser," *Electron. Lett.* **29**, 1860–1861 (1993).
59. P. V. Mamyshev, S. V. Chernikov, and E. M. Dianov, "Generation of fundamental soliton trains for high bit-rate optical fiber communication lines," *IEEE J. Quantum Electron.* **27**, 2347–2355 (1991).
60. B. C. Stuart, M. D. Feit, A. M. Rubenchik, B. W. Shore, and M. D. Perry, "Laser induced damage in dielectrics with nanosecond to subpicosecond pulses," *Phys. Rev. Lett.* **74**, 2248–2251 (1995).
61. B. C. Stuart, M. D. Feit, S. Herman, A. M. Rubenchik, B. W. Shore, and M. D. Perry, "Nanosecond-to-femtosecond laser-induced breakdown in dielectrics," *Phys. Rev. B* **53**, 1749–1761 (1996).
62. R. L. Farrow, D. A. V. Kliner, G. R. Hadley, and A. V. Smith, "Peak power limits on fiber amplifiers imposed by self-focusing," *Opt. Lett.* **31**, 3423–3425 (2006).
63. D. P. Hand and P. S. Russell, "Solitary thermal-shock waves and optical damage in optical fibers—the fiber fuse," *Opt. Lett.* **13**, 767–769 (1988).
64. H. L. Offerhaus, N. G. Broderick, D. J. Richardson, R. Sammut, J. Caplen, and L. Dong, "High-energy single-transverse-mode Q-switched fiber laser based on a multi-mode large-mode-area erbium-doped fiber," *Opt. Lett.* **23**, 1683–1685 (1998).
65. A. Piper, A. Malinowski, K. Furusawa, and D. J. Richardson, "High-power high-brightness mJ Q-switched ytterbium-doped fiber laser," *Electron. Lett.* **40**, 928–929 (2004).
66. O. Schmidt, J. Rothhardt, F. Röser, S. Linke, T. Schreiber, K. Rademaker, J. Limpert, S. Ermenoux, P. Yvernault, F.

- Salin, and A. Tünnermann, "Millijoule pulse energy Q-switched short-length fiber laser," *Opt. Lett.* **32**, 1551–1553 (2007).
67. T. V. Andersen, P. Perez-Millan, S. R. Keiding, S. Agger, R. Duchowicz, and M. V. Andres, "All-fiber actively Q-switched Yb-doped laser," *Opt. Commun.* **260**, 251–256 (2006).
 68. M. Delgado-Pinar, D. Zalvidea, A. Diez, P. Perez-Millan, and M. V. Andres, "Q-switching of an all-fiber laser by acousto-optic modulation of a fiber Bragg grating," *Opt. Express* **14**, 1106–1112 (2006).
 69. M. L. R. Laroche, A. M. Chardon, J. Nilsson, D. P. Shepherd, W. A. Clarkson, S. Girard, and R. Moncorgé, "Compact diode-pumped passively Q-switched tunable Er-Yb double-clad fiber laser," *Opt. Lett.* **27**, 1980–1982 (2002).
 70. L. Pan, I. Utkin, and R. Fedosejevs, "Passively Q-switched ytterbium-doped double-clad fiber laser with a Cr⁴⁺:YAG saturable absorber," *IEEE Photon. Technol. Lett.* **19**, 1979–1981 (2007).
 71. J. B. Lecourt, G. Martel, M. Guezo, C. Labbe, and S. Loualiche, "Erbium-doped fiber laser passively Q-switched by an InGaAs/InP multiple quantum well saturable absorber," *Opt. Commun.* **263**, 71–83 (2006).
 72. R. Paschotta, R. Haring, E. Gini, H. Melchior, U. Keller, H. L. Offerhaus, and D. J. Richardson, "Passively Q-switched 0.1-mJ fiber laser system at 1.53 μm ," *Opt. Lett.* **24**, 388–390 (1999).
 73. J. Nilsson and B. Jaskorzynska, "Modeling and optimization of low-repetition-rate high-energy pulse amplification in cw-pumped erbium-doped fiber amplifiers," *Opt. Lett.* **18**, 2099–2101 (1993).
 74. M. Y. Cheng, Y. C. Chang, A. Galvanauskas, P. Mamidipudi, R. Changkakoti, and P. Gatchell, "High-energy and high-peak-power nanosecond pulse generation with beam quality control in 200- μm core highly multimode Yb-doped fiber amplifiers," *Opt. Lett.* **30**, 358–360 (2005).
 75. B. Desthieux, R. I. Laming, and D. N. Payne, "111 kW (0.5 mJ) pulse amplification at 1.5- μm using a gated cascade of 3 erbium-doped fiber amplifiers," *Appl. Phys. Lett.* **63**, 586–588 (1993).
 76. J. Limpert, S. Höfer, A. Liem, H. Zellmer, A. Tünnermann, S. Knoke, and H. Voelckel, "100-W average-power high-energy nanosecond fiber amplifier," *Appl. Phys. B* **75**, 477–479 (2002).
 77. K. T. Vu, A. Malinowski, D. J. Richardson, F. Ghiringhelli, L. M. B. Hickey, and M. N. Zervas, "Adaptive pulse shape control in a diode seeded nanosecond fiber MOPA system," *Opt. Express* **14**, 10996–11001 (2006).
 78. D. N. Schimpf, C. Ruchert, D. Nodop, J. Limpert, A. Tünnermann, and F. Salin, "Compensation of pulse-distortion in saturated laser amplifiers," *Opt. Express* **16**, 17637–17646 (2008).
 79. A. Malinowski, K. T. Vu, K. K. Chen, J. Nilsson, Y. Jeong, S. Alam, D. J. Lin, and D. J. Richardson, "High power pulsed fiber MOPA system incorporating electro-optic modulator based adaptive pulse shaping," *Opt. Express* **17**, 20927–20937 (2009).
 80. D. Lin, S. U. Alam, K. K. Chen, A. Malinowski, S. Norman, and D. J. Richardson, "100 W fully fiberised ytterbium doped master oscillator power amplifier incorporating adaptive pulse shaping," in *Proceedings of the Conference on Lasers and Electro Optics*, 2009 OSA Technical Digest Series (Optical Society of America, 2009), paper CFM4.
 81. C. D. Brooks and F. Di Teodoro, "Multimegawatt peak-power, single-transverse-mode operation of a 100 μm core diameter, Yb-doped rod-like photonic crystal fiber amplifier," *Appl. Phys. Lett.* **89**, 111119 (2006).
 82. G. Krauss, S. Lohss, T. Hanke, A. Sell, S. Eggert, R. Huber, and A. Leitenstorfer, "Synthesis of a single cycle of light with compact erbium-doped fibre technology," *Nat. Photonics* **4**, 33–36 (2010).
 83. T. Schreiber, C. K. Nielsen, B. Ortac, and J. Limpert, "Microjoule-level all-polarization-maintaining femtosecond fiber source," *Opt. Lett.* **31**, 574–576 (2006).
 84. L. Dong, H. A. McKay, L. B. Fu, M. Ohta, A. Marcinkevicius, S. Suzuki, and M. E. Fermann, "Ytterbium-doped all glass leakage channel fibers with highly fluorine-doped silica pump cladding," *Opt. Express* **17**, 8962–8969 (2009).
 85. P. Dupriez, A. Piper, A. Malinowski, J. K. Sahu, M. Ibsen, B. C. Thomsen, Y. Jeong, L. M. B. Hickey, M. N. Zervas, J. Nilsson, and D. J. Richardson, "High average power, high repetition rate, picosecond pulsed fiber master oscillator power amplifier source seeded by a gain-switched laser diode at 1060 nm," *IEEE Photon. Technol. Lett.* **18**, 1013–1015 (2006).
 86. K. K. Chen, S. U. Alam, J. R. Hayes, H. J. Baker, D. Hall, R. McBride, J. H. V. Price, D. J. Lin, A. Malinowski, and D. J. Richardson, "56-W frequency-doubled source at 530 nm pumped by a single-mode, single-polarization, picosecond, Yb³⁺-doped fiber MOPA," *IEEE Photon. Technol. Lett.* **22**, 893–895 (2010).
 87. K. K. Chen, S. U. Alam, J. H. V. Price, J. R. Hayes, D. J. Lin, A. Malinowski, and D. J. Richardson, "Picosecond fiber MOPA pumped supercontinuum source with 39 W output power," *Opt. Express* **18**, 5426–5432 (2010).
 88. F. Kienle, K. K. Chen, S.-U. Alam, C. B. E. Gawith, J. I. McKenzie, D. C. Hanna, D. J. Richardson, and D. P. Shepherd, "High-power, variable repetition rate, picosecond optical parametric oscillator pumped by an amplified gain-switched diode," *Opt. Express* **18**, 7602–7610 (2010).
 89. T. Eidam, S. Hanf, E. Seise, T. V. Andersen, T. Gabler, C. Wirth, T. Schreiber, J. Limpert, and A. Tünnermann, "Femtosecond fiber CPA system emitting 830 W average output power," *Opt. Lett.* **35**, 94–96 (2010).
 90. J. M. Dudley, C. Finot, D. J. Richardson, and G. Millot, "Self-similarity in ultrafast nonlinear optics," *Nat. Phys.* **3**, 597–603 (2007).
 91. M. E. Fermann, V. I. Kruglov, B. C. Thomsen, J. M. Dudley, and J. D. Harvey, "Self-similar propagation and amplification of parabolic pulses in optical fibers," *Phys. Rev. Lett.* **84**, 6010–6013 (2000).
 92. A. Malinowski, A. Piper, J. H. V. Price, K. Furusawa, Y. Jeong, J. Nilsson, and D. J. Richardson, "Ultrashort-pulse Yb³⁺-fiber-based laser and amplifier system producing >25-W average power," *Opt. Lett.* **29**, 2073–2075 (2004).
 93. J. Limpert, T. Schreiber, T. Clausnitzer, L. Zollner, H. J. Fuchs, E. B. Kley, H. Zellmer, and A. Tünnermann, "High-power femtosecond Yb-doped fiber amplifier," *Opt. Express* **10**, 628–638 (2002).
 94. D. Strickland and G. Mourou, "Compression of amplified chirped optical pulses," *Opt. Commun.* **56**, 219–221 (1985).
 95. M. E. Fermann, A. Galvanauskas, G. Sucha, and D. Harter, "Fiber-lasers for ultrafast optics," *Appl. Phys. B* **65**, 259–275 (1997).
 96. F. Röser, T. Eidam, J. Rothhardt, O. Schmidt, D. N. Schimpf, J. Limpert, and A. Tünnermann, "Millijoule pulse energy high repetition rate femtosecond fiber chirped-pulse amplification system," *Opt. Lett.* **32**, 3495–3497 (2007).
 97. J. Limpert, F. Röser, D. N. Schimpf, E. Seisse, T. Eidam, S. Hädrich, L. Rothhardt, C. Jauregui Misas, and A. Tünnermann, "High repetition rate gigawatt peak power fiber laser-systems: Challenges, design, and experiment," *IEEE J. Sel. Top. Quantum Electron.* **15**, 159–169 (2009).
 98. C. J. S. de Matos, J. R. Taylor, T. P. Hansen, K. P. Hansen, and J. Broeng, "All-fiber chirped pulse amplification using highly-dispersive air-core photonic bandgap fiber," *Opt. Express* **11**, 2832–2837 (2003).
 99. J. Nilsson, W. A. Clarkson, R. Selvas, J. K. Sahu, P. W. Turner, S. U. Alam, and A. B. Grudinin, "High-power wavelength-tunable cladding-pumped rare-earth-doped silica fiber lasers," *Opt. Fiber Technol.* **10**, 5–30 (2004).
 100. J. E. Townsend, W. L. Barnes, K. P. Jdrzejewski, and S. G. Grubb, "Yb sensitised Er doped silica optical fiber with ultrahigh transfer efficiency and gain," *Electron. Lett.* **27**, 1958–1959 (1991).
 101. J. Nilsson, S. U. Alam, J. A. Alvarez-Chavez, P. W. Turner, W. A. Clarkson, and A. B. Grudinin, "High-power and tunable operation of erbium-ytterbium co-doped cladding-pumped fiber laser," *IEEE J. Quantum Electron.* **39**, 987–994 (2003).
 102. C. Codemard, D. B. S. Soh, K. Ylä-Jarkko, J. K. Sahu, M.

- Laroche, and J. Nilsson, "Cladding-pumped L-band phosphosilicate erbium-ytterbium co-doped fiber amplifier," in *Optical Amplifiers and Their Applications*, 2003 OSA Technical Digest Series (Optical Society of America, 2003), paper TuC2.
103. Y. Jeong, S. Yoo, C. A. Codemard, J. Nilsson, J. K. Sahu, D. N. Payne, R. Horley, P. W. Turner, L. M. B. Hickey, A. Harker, M. Lovelady, and A. Piper, "Erbium:ytterbium co-doped large-core fiber laser with 297 W continuous-wave output power," *IEEE J. Sel. Top. Quantum Electron.* **13**, 573–579 (2007).
 104. A. Yusim, J. Barsalou, D. Gapontsev, N. S. Platonov, O. Shkurikhin, V. P. Gapontsev, Y. A. Barannikov, and F. V. Shcherbina, "100 watt single-mode CW linearly polarized all-fiber format 1.56- μm laser with suppression of parasitic lasing effects," *Proc. SPIE* **5709**, 69–77 (2005).
 105. D. Y. Shen, J. K. Sahu, and W. A. Clarkson, "Highly efficient Er:Yb-doped fiber laser with 188 W free-running and >100 W tunable output power," *Opt. Express* **13**, 4916–4921 (2005).
 106. G. Canat, J. C. Mollier, Y. Jaouen, and B. Dussardier, "Evidence of thermal effects in a high-power Er³⁺-Yb³⁺ fiber laser," *Opt. Lett.* **30**, 3030–3032 (2005).
 107. M. A. Lapointe, S. Chatigny, M. Piché, M. Cain-Skaff, and J.-N. Maran, "Thermal effects in high-power CW fiber lasers," *Proc. SPIE* **7195**, 71951U (2009).
 108. J. W. Kim, D. Y. Shen, J. K. Sahu, and W. A. Clarkson, "Fiber-laser-pumped Er:YAG lasers," *IEEE J. Sel. Top. Quantum Electron.* **15**, 361–371 (2009).
 109. M. Dubinskii, J. Zhang, and V. Ter-Mikirtychev, "Highly scalable, resonantly cladding-pumped, Er-doped fiber laser with record efficiency," *Opt. Lett.* **34**, 1507–1509 (2009).
 110. J. W. Nicholson, A. M. DeSantolo, S. Ghalmi, J. M. Fini, J. Fleming, E. Monberg, F. DiMarcello, and S. Ramachandran, "Nanosecond pulse amplification in a higher-order-mode erbium-doped fiber amplifier," in *Proceedings of the Conference on Lasers and Electro-Optics*, 2010 OSA Technical Digest Series (Optical Society of America, 2010), paper CPDB5.
 111. S. D. Jackson, "The spectroscopic and energy transfer characteristics of rare earth ions used for silicate glass fibre lasers operating in the shortwave infrared," *Laser Photonics Rev.* **3**, 466–482 (2009).
 112. D. Y. Shen, J. K. Sahu, and W. A. Clarkson, "High-power widely tunable Tm: fibre lasers pumped by an Er, Yb co-doped fibre laser at 1.6 microns," *Opt. Express* **14**, 6084–6090 (2006).
 113. M. Meleshkevich, N. Platonov, D. V. Gapontsev, A. Drozhzhin, V. P. Gapontsev, and V. Sergeev, "415 W single-mode CW thulium fiber laser in all-fiber format," in *Proceedings of the European Conference on Lasers and Electro-Optics* (2007), post-deadline paper CP-2-3-THU.
 114. T. Y. Fan, G. Huber, R. L. Byer, and P. Mitzscherlich, "Spectroscopy and diode laser-pumped operation of Tm:Ho:YAG," *IEEE J. Quantum Electron.* **24**, 924–933 (1988).
 115. R. A. Hayward, W. A. Clarkson, P. W. Turner, J. Nilsson, A. B. Grudinin, and D. C. Hanna, "Efficient cladding-pumped Tm-doped silica fibre laser with high power single mode output at 2 μm ," *Electron. Lett.* **36**, 711–712 (2000).
 116. S. D. Jackson, "Cross relaxation and energy transfer up-conversion processes relevant to the functioning of 2 μm Tm³⁺ doped silica fibre lasers," *Opt. Commun.* **230**, 197–203 (2004).
 117. P. F. Moulton, G. A. Rines, E. V. Slobodtchikov, K. F. Wall, G. Firth, B. Samson, and A. L. G. Carter, "Tm-doped fiber lasers: Fundamentals and power scaling," *IEEE J. Sel. Top. Quantum Electron.* **15**, 85–92 (2009).
 118. T. Ehrenreich, R. Leveille, I. Majid, K. Tankala, G. Rines, and P. F. Moulton, "1-kW, all-glass Tm: fiber laser," in *Fiber Lasers VII: Technology, Systems, and Applications* (2010) (Session 16: Late breaking news).
 119. L. Pearson, J. W. Kim, Z. Zhang, M. Ibsen, J. K. Sahu, and W. A. Clarkson, "High-power linearly-polarized single-frequency thulium-doped fiber master-oscillator power amplifier," *Opt. Express* **18**, 1607–1612 (2010).
 120. G. D. Goodno, L. D. Book, and J. E. Rothenberg, "Low-phase-noise, single-frequency, single-mode 608 W thulium fiber amplifier," *Opt. Lett.* **34**, 1204–1206 (2009).
 121. S. D. Jackson, "Midinfrared holmium fiber laser," *IEEE J. Quantum Electron.* **42**, 187–191 (2006).
 122. S. D. Jackson, A. Sabella, A. Hemming, S. Bennetts, and D. G. Lancaster, "High-power 83 W holmium-doped silica fiber laser operating with high beam quality," *Opt. Lett.* **32**, 241–243 (2007).
 123. D. J. DiGiovanni and A. J. Stentz, "Tapered fiber bundles for coupling light into and out of cladding-pumped fiber devices," U.S. patent 5,864,644 (26 January 1999).
 124. See IPG website at <http://www.ipgphotonics.com>.
 125. T. Y. Fan, "Laser beam combining for high-power, high-radiance sources," *IEEE J. Sel. Top. Quantum Electron.* **11**, 567–577 (2005).
 126. O. Andrusyak, V. Smirnov, G. Venus, V. Rotar, and L. Glebov, "Spectral combining and coherent coupling of lasers by volume Bragg gratings," *IEEE J. Sel. Top. Quantum Electron.* **15**, 344–353 (2009).
 127. M. Engholm, "Materials optimization for optical fiber amplifiers and fiber lasers," Ph.D. dissertation (Mid Sweden University, 2008).
 128. C. A. Codemard, A. Shirakawa, J. K. Sahu, S. Yoo, Y. Jeong, and J. Nilsson, "Thermal resilience of polymer-coated double-clad fiber," in *Proceedings of the European Conference on Lasers and Electro Optics* (2009), paper CJ.P.5.
 129. D. C. Brown and H. J. Hoffmann, "Thermal, stress, and thermo-optic effects in high average power double-clad silica fiber lasers," *IEEE J. Quantum Electron.* **37**, 207–217 (2001).
 130. See PolyMicro website at http://www.polymicro.com/products/opticalfibers/products_opticalfibers_fsu_flu.htm.
 131. K. Furusawa, A. Malinowski, J. H. V. Price, T. M. Monro, J. K. Sahu, J. Nilsson, and D. J. Richardson, "Cladding pumped ytterbium-doped fiber laser with holey inner and outer cladding," *Opt. Express* **9**, 714–720 (2001).
 132. W. J. Wadsworth, R. M. Percival, G. Bouwmans, J. C. Knight, T. A. Birks, T. D. Hedley, and P. St. J. Russell, "Very high numerical aperture fibers," *IEEE Photon. Technol. Lett.* **16**, 843–845 (2004).
 133. J. Limpert, T. Schreiber, A. Liem, S. Nolte, H. Zellmer, T. Peschel, V. Guyenot, and A. Tünnermann, "Thermo-optical properties of air-clad photonic crystal fiber lasers in high power operation," *Opt. Express* **11**, 2982–2990 (2003).
 134. T. Schreiber, C. Hagemann, J. K. Kim, T. Peschel, and S. Böhme, *Annual Report* (Fraunhofer-Institut für Angewandte Optik und Feinmechanik, 2009), p. 105.
 135. Y. Feng, L. R. Taylor, and D. Bonaccini Calia, "150 W highly-efficient Raman fiber laser," *Opt. Express* **17**, 23678–23683 (2009).
 136. C. A. Codemard, J. Ji, J. K. Sahu, and J. Nilsson, "100 W CW cladding-pumped Raman fiber laser at 1120 nm," *Proc. SPIE* **7580**, 75801N (2010).
 137. B. Steinhauser, A. Brignon, E. Lallier, J. P. Huignard, and P. Georges, "High energy, single-mode, narrow-linewidth fiber laser source using stimulated Brillouin scattering beam cleanup," *Opt. Express* **15**, 6464–6469 (2007).
 138. D. Nodop, C. Jauregui, D. Schimpf, J. Limpert, and A. Tünnermann, "Efficient high-power generation of visible and mid-infrared light by degenerate four-wave-mixing in a large-mode-area photonic-crystal fiber," *Opt. Lett.* **34**, 3499–3501 (2009).
 139. W. Torruellas, Y. Chen, B. McIntosh, J. Farroni, K. Tankala, S. Webster, D. Hagan, M. J. Soileau, M. Messerly, and J. Dawson, "High peak power ytterbium-doped fiber amplifiers," *Proc. SPIE* **6102**, 61020N (2006).
 140. A. V. Smith and B. T. Do, "Bulk and surface laser damage of silica by picosecond and nanosecond pulses at 1064 nm," *Appl. Opt.* **47**, 4812–4832 (2008).
 141. M. Efimov, "Intrinsic laser-induced damage in bulk transparent dielectrics," in *Proceedings of the Conference on Lasers and Electro-Optics*, 2010 OSA Technical Digest Series (Optical Society of America, 2010), paper CFG1.

142. J. W. Dawson, R. Beach, I. Jovanovic, B. Wattellier, Z. Liao, S. Payne, and C. P. J. Barty, "Large flattened mode optical fiber for reduction of nonlinear effects in optical fiber lasers," *Proc. SPIE* **5335**, 132–139 (2004).
143. M. E. Fermann, "Single-mode excitation of multimode fibers with ultrashort pulses," *Opt. Lett.* **23**, 52–54 (1998).
144. N. G. R. Broderick, H. L. Offerhaus, D. J. Richardson, R. A. Sammut, J. Caplen, and L. Dong, "Large mode area fibers for high power applications," *Opt. Fiber Technol.* **5**, 185–196 (1999).
145. J. M. Sousa and O. G. Okhotnikov, "Multimode Er-doped fiber for single-transverse-mode amplification," *Appl. Phys. Lett.* **74**, 1528–1530 (1999).
146. J. P. Koplow, D. A. V. Kliner, and L. Goldberg, "Single-mode operation of a coiled multimode fiber amplifier," *Opt. Lett.* **25**, 442–444 (2000).
147. S. Ramachandran, J. M. Fini, M. Mermelstein, J. W. Nicholson, S. Ghalmi, and M. F. Yan, "Ultra-large effective-area, higher-order mode fibers: a new strategy for high-power lasers," *Laser Photonics Rev.* **2**, 429–448 (2008).
148. S. H. Huang, C. Zhu, C. H. Liu, X. Q. Ma, C. Swan, and A. Galvanauskas, "Power scaling of CCC fiber based lasers," in *Proceedings of the Conference on Lasers and Electro-Optics*, 2009 OSA Technical Digest Series (Optical Society of America, 2009), pp. 988–989.
149. O. Schmidt, J. Rothhardt, T. Eidam, F. Röser, J. Limpert, A. Tünnermann, K. P. Hansen, C. Jakobsen, and J. Broeng, "Single-polarization ultra-large-mode-area Yb-doped photonic crystal fiber," *Opt. Express* **16**, 3918–3923 (2008).
150. K. P. Hansen, C. B. Olausson, J. Broeng, K. Mattsson, M. D. T. Nikolajsen, P. M. W. Skovgaard, M. H. Sorensen, M. Denninger, C. Jakobsen, and H. R. Simonsen, "Aircad fiber laser technology," *Proc. SPIE* **6873**, U3–U14 (2008).
151. L. Dong, H. A. McKay, A. Marcinkevicius, L. B. Fu, J. Li, B. K. Thomas, and M. E. Fermann, "Extending effective area of fundamental mode in optical fibers," *J. Lightwave Technol.* **27**, 1565–1570 (2009).
152. V. Sudesh, T. McComb, Y. Chen, M. Bass, M. Richardson, J. Ballato, and A. E. Siegman, "Diode-pumped 200 μm diameter core, gain-guided, index-antiguidded single mode fiber laser," *Appl. Phys. B* **90**, 369–372 (2008).
153. X. Zhu, A. Schülzgen, H. Li, L. Li, Q. Wang, S. Suzuki, V. L. Temyanko, J. V. Moloney, and N. Peyghambarian, "Single-transverse-mode output from a fiber laser based on multimode interference," *Opt. Lett.* **33**, 908–910 (2008).
154. M. Paurisse, M. Hanna, F. Druon, P. Georges, C. Bellanger, A. Brignon, and J. P. Huignard, "Phase and amplitude control of a multimode LMA fiber beam by use of digital holography," *Opt. Express* **17**, 13000–13008 (2009).
155. C. A. Codemard, J. Nilsson, and J. K. Sahu, "Tandem pumping of large-core double-clad Ytterbium-doped fiber for control of excess gain," in *Advanced Solid State Photonics*, 2010 OSA Technical Digest Series (Optical Society of America, 2010), paper AWA3.
156. J. Nilsson, "High power fiber lasers and amplifiers," in *Optical Fiber Communications Conference*, 2007 OSA Technical Digest Series (Optical Society of America, 2007), short course SC 290.
157. R. T. Schermer, "Mode scalability in bent optical fibers," *Opt. Express* **15**, 15674–15701 (2007).
158. J. R. Marciante, R. G. Roides, V. V. Shkunov, and D. A. Rockwell, "Near-diffraction-limited operation of step-index large-mode-area fiber lasers via gain filtering," *Opt. Lett.* **35**, 1828–1830 (2010).
159. J. C. Jasapara, M. J. Andrejco, A. DeSantolo, A. D. Yablon, Z. Varallyay, J. W. Nicholson, J. M. Fini, D. J. DiGiovanni, C. Headley, E. Monberg, and F. V. DiMarcello, "Diffraction-limited fundamental mode operation of core-pumped very-large-mode-area Er fiber amplifiers," *IEEE J. Sel. Top. Quantum Electron.* **15**, 3–11 (2009).
160. J. W. Dawson, M. J. Messerly, R. J. Beach, M. Y. Shverdin, E. A. Stappaerts, A. K. Sridharan, P. H. Pax, J. E. Heebner, C. W. Siders, and C. P. J. Barty, "Analysis of the scalability of diffraction-limited fiber lasers and amplifiers to high average power," *Opt. Express* **16**, 13240–13266 (2008).
161. R. F. Cregan, B. J. Mangan, J. C. Knight, T. A. Birks, P. S. Russell, P. J. Roberts, and D. C. Allan, "Single-mode photonic band gap guidance of light in air," *Science* **285**, 1537–1539 (1999).
162. F. Couny, F. Benabid, and P. S. Light, "Large-pitch kagome-structured hollow-core photonic crystal fiber," *Opt. Lett.* **31**, 3574–3576 (2006).
163. F. Couny, F. Benabid, and P. S. Light, "Subwatt threshold cw Raman fiber-gas laser based on H₂-filled hollow-core photonic crystal fiber," *Phys. Rev. Lett.* **99**, 143903 (2007).
164. E. M. Dianov, M. E. Likhachev, and S. Fevrier, "Solid-core photonic bandgap fibers for high-power fiber lasers," *IEEE J. Sel. Top. Quantum Electron.* **15**, 20–29 (2009).
165. A. Shirakawa, H. Maruyama, K. Ueda, C. B. Olausson, J. K. Lyngsø, and J. Broeng, "High-power Yb-doped photonic bandgap fiber amplifier at 1150–1200 nm," *Opt. Express* **17**, 447–454 (2009).
166. H. Lee and G. Agrawal, "Suppression of stimulated Brillouin scattering in optical fibers using fiber Bragg gratings," *Opt. Express* **11**, 3467–3472 (2003).
167. P. Sprangle, A. Ting, J. Penano, R. Fischer, and B. Hafizi, "Incoherent combining and atmospheric propagation of high-power fiber lasers for directed-energy applications," *IEEE J. Quantum Electron.* **45**, 138–148 (2009).
168. S. J. Augst, J. K. Ranka, T. Y. Fan, and A. Sanchez, "Beam combining of ytterbium fiber amplifiers," *J. Opt. Soc. Am. B* **24**, 1707–1715 (2007).
169. O. Schmidt, C. Wirth, I. Tsybin, T. Schreiber, R. Eberhardt, J. Limpert, and A. Tünnermann, "Average power of 1.1 kW from spectrally combined, fiber-amplified, nanosecond-pulsed sources," *Opt. Lett.* **34**, 1567–1569 (2009).
170. A. Shirakawa, T. Saitou, T. Sekiguchi, and K. Ueda, "Coherent addition of fiber lasers by use of a fiber coupler," *Opt. Express* **10**, 1167–1172 (2002).
171. M. L. Minden, H. Bruesselbach, J. L. Rogers, M. S. Mangir, D. C. Jones, G. J. Dunning, D. L. Hammon, A. J. Solis, and L. Vaughan, "Self-organized coherence in fiber laser arrays," *Proc. SPIE* **5335**, 89–97 (2004).
172. C. J. Corcoran and F. Durville, "Experimental demonstration of a phase-locked laser array using a self-Fourier cavity," *Appl. Phys. Lett.* **86**, 201118 (2005).
173. J. R. Leger, G. J. Swanson, and W. B. Veldkamp, "Coherent laser addition using binary phase gratings," *Appl. Opt.* **26**, 4391–4399 (1987).
174. L. Li, A. Schülzgen, H. Li, V. L. Temyanko, J. V. Moloney, and N. Peyghambarian, "Phase-locked multicore all-fiber lasers: modeling and experimental investigation," *J. Opt. Soc. Am. B* **24**, 1721–1728 (2007).
175. D. Kouznetsov, J. Bisson, A. Shirakawa, and K. Ueda, "Limits of coherent addition of lasers: Simple estimate," *Opt. Rev.* **12**, 445–447 (2005).
176. J. E. Rothenberg, "Passive coherent phasing of fiber laser arrays," *Proc. SPIE* **6873**, 687315 (2008).
177. W. Chang, H. G. Winful, and A. Galvanauskas, "Array size scalability of passively coherently phased fiber laser arrays," *Opt. Express* **18**, 9634–9642 (2010).
178. M. Khajavikhan, K. John, and J. R. Leger, "Experimental measurements of supermodes in superposition architectures for coherent laser beam combining," *IEEE J. Quantum Electron.* **46**, 1221–1231 (2010).
179. E. J. Bochove, P. K. Cheo, and G. G. King, "Self-organization in a multicore fiber laser array," *Opt. Lett.* **28**, 1200–1202 (2003).
180. C. J. Corcoran, F. Durville, and K. A. Pasch, "Coherent array of nonlinear regenerative fiber amplifiers," *IEEE J. Quantum Electron.* **44**, 275–282 (2008).
181. F. Kong, L. Liu, C. Sanders, Y. C. Chen, and K. K. Lee, "Phase locking of nanosecond pulses in a passively Q-switched two-element fiber laser array," *Appl. Phys. Lett.* **90**, 151110 (2007).

182. R. Uberna, A. Bratcher, T. G. Alley, A. D. Sanchez, A. S. Flores, and B. Pulford, "Coherent combination of high power fiber amplifiers in a two-dimensional re-imaging waveguide," *Opt. Express* **18**, 13547–13553 (2010).
183. E. C. Cheung, J. G. Ho, G. D. Goodno, R. R. Rice, J. Rothenberg, P. Thielen, M. Weber, and M. Wickham, "Diffractive-optics-based beam combination of a phase-locked fiber laser array," *Opt. Lett.* **33**, 354–356 (2008).
184. T. M. Shay, V. Benham, J. T. Baker, A. D. Sanchez, D. Pilkington, and C. A. Lu, "Self-synchronous and self-referenced coherent beam combination for large optical arrays," *IEEE J. Sel. Top. Quantum Electron.* **13**, 480–486 (2007).
185. X. H. Fang, M. L. Hu, B. W. Liu, L. Chai, C. Y. Wang, and A. M. Zheltikov, "Generation of 150 MW, 110 fs pulses by phase-locked amplification in multicore photonic crystal fiber," *Opt. Lett.* **35**, 2326–2328 (2010).
186. I. Hartl, H. A. McKay, A. Marcinkevicius, L. Dong, and M. E. Fermann, "Multi-core leakage-channel fibers with up to 26000 μm^2 combined effective mode-field area," in *Proceedings of the Conference on Lasers and Electro-Optics*, Vols. 1–5 of 2009 OSA Technical Digest Series (Optical Society of America, 2009), pp. 1684–1685.
187. J. Limpert, N. Deguil-Robin, I. Manek-Hönniger, F. Salin, T. Schreiber, A. Liem, F. Röser, H. Zellmer, A. Tünnermann, A. Courjaud, C. Hönniger, and E. Mottay, "High-power picosecond fiber amplifier based on nonlinear spectral compression," *Opt. Lett.* **30**, 714–716 (2005).
188. K. K. Chen, S. Alam, P. Horak, C. Codemard, A. Malinowski, and D. J. Richardson, "Excitation of individual Raman orders in the visible using rectangular pulses," *Opt. Lett.* **35**, 2433–2435 (2010).
189. P. Petropoulos, M. Ibsen, A. D. Ellis, and D. J. Richardson, "Rectangular pulse generation based on pulse reshaping using a superstructured fiber Bragg grating," *J. Lightwave Technol.* **19**, 746–752 (2001).
190. R. Slavik, Y. Park, and J. Azana, "Long-period fiber-grating-based filter for generation of picosecond and sub-picosecond transform-limited flat-top pulses," *IEEE Photon. Technol. Lett.* **20**, 806–808 (2008).
191. See Finisar website at www.finisar-systems.com/download_53KDmt10500001-1050004-WaveShaper-Family-product-brief-RevB.pdf.
192. V. V. Dvoyrin, A. V. Kir'yanov, V. M. Mashinsky, O. I. Medvedkov, A. A. Umnikov, A. N. Guryanov, and E. M. Dianov, "Absorption, gain, and laser action in bismuth-doped aluminosilicate optical fibers," *IEEE J. Quantum Electron.* **46**, 182–190 (2010).
193. E. M. Dianov, "Bi-doped glass optical fibers: Is it a new breakthrough in laser materials?" *J. Non-Cryst. Solids* **355**, 1861–1864 (2009).
194. S. Yoo, M. P. Kalita, A. J. Boyland, A. S. Webb, R. J. Standish, J. K. Sahu, M. C. Paul, S. Das, S. K. Bhadra, and M. Pal, "Ytterbium-doped Y_2O_3 nanoparticle silica optical fibers for high power fiber lasers with suppressed photodarkening," *Opt. Commun.* **283**, 3423–3427 (2010).
195. J. Adam, "Fluoride glass research in France: fundamentals and applications," *J. Fluorine Chem.* **107**, 265–270 (2001).
196. M. D. O'Donnell, C. A. Miller, D. Furniss, V. K. Tikhomirov, and A. B. Seddon, "Fluorotellurite glasses with improved mid-infrared transmission," *J. Non-Cryst. Solids* **331**, 48–57 (2003).
197. J. Sanghera, L. B. Shaw, and I. D. Aggarwal, "Chalcogenide glass-fiber-based mid-IR sources and applications," *IEEE J. Sel. Top. Quantum Electron.* **15**, 114–119 (2009).
198. S. D. Jackson, "High-power and highly-efficient diode-cladding-pumped holmium-doped fluoride fiber laser at 2.94 μm ," *Opt. Lett.* **34**, 2327–2329 (2009).
199. M. Pollnau and S. D. Jackson, "Erbium 3- μm fiber lasers," *IEEE J. Sel. Top. Quantum Electron.* **7**, 30–40 (2001).
200. S. Tokita, M. Murakami, S. Shimizu, M. Hashida, and S. Sakabe, "Liquid-cooled 24 W mid-infrared Er:ZBLAN fiber laser," *Opt. Lett.* **34**, 3062–3064 (2009).
201. I. S. Moskalev, V. V. Fedorov, and S. B. Mirov, "10-Watt, pure continuous-wave, polycrystalline Cr^{2+} :ZnSe laser," *Opt. Express* **17**, 2048–2056 (2009).
202. T. J. Carrig, "Transition-metal-doped chalcogenide lasers," *J. Electron. Mater.* **31**, 759–769 (2002).
203. V. V. Fedorov, S. B. Mirov, A. Gallian, D. V. Badikov, M. P. Frolov, Y. V. Korostelin, V. I. Kozlovsky, A. I. Landman, Y. P. Podmar'kov, V. A. Akimov, and A. A. Voronov, "3.77–5.05- μm tunable solid-state lasers based on Fe^{2+} -doped ZnSe crystals operating at low and room temperatures," *IEEE J. Quantum Electron.* **42**, 907–917 (2006).
204. P. A. Champert, S. V. Popov, J. R. Taylor, and J. P. Meyn, "Efficient second-harmonic generation at 384 nm in periodically poled lithium tantalate by use of a visible Yb-Er-seeded fiber source," *Opt. Lett.* **25**, 1252–1254 (2000).
205. P. A. Champert, S. V. Popov, and J. R. Taylor, "Power scalability to 6 W of 770 nm source based on seeded fibre amplifier and PPKTP," *Electron. Lett.* **37**, 1127–1129 (2001).
206. Y. Shen, S. U. Alam, K. K. Chen, D. J. Lin, S. Cai, B. Wu, P. Jiang, A. Malinowski, and D. J. Richardson, "PPMgLN based high power optical parametric oscillator pumped by Yb^{3+} -doped fiber amplifier incorporating active pulse shaping," *IEEE J. Sel. Top. Quantum Electron.* **15**, 385–392 (2009).
207. P. Dupriez, J. K. Sahu, A. Malinowski, Y. Jeong, D. J. Richardson, and J. Nilsson, "80 W green laser based on a frequency-doubled picosecond single-mode linearly-polarized fiber laser," in *Proceedings of the Conference on Lasers and Electro-Optics*, 2006 OSA Technical Digest Series (Optical Society of America, 2006), paper CThJ1.